RSC Advances

PAPER

View Article Online
View Journal | View Issue

Cite this: *RSC Adv.*, 2020, **10**, 12272

Seeking potent anti-tubercular agents: design and synthesis of substituted-*N*-(6-(4-(pyrazine-2-carbonyl)piperazine/homopiperazine-1-yl)pyridin-3-yl)benzamide derivatives as anti-tubercular agents†

Singireddi Srinivasarao,[a] Adinarayana Nandikolla,[a] Amaroju Suresh,[a] Kevin Van Calster,[b] Linda De Voogt,[b] Davie Cappoen,[b] Balaram Ghosh,[c] Himanshu Aggarwal,[a] Sankaranarayanan Murugesan[d] and Kondapalli Venkata Gowri Chandra Sekhar *[a]

Received 12th February 2020
Accepted 18th March 2020

DOI: 10.1039/d0ra01348j

rsc.li/rsc-advances

Pyrazinamide is an important first-line drug used in shortening TB therapy. In our current work, a series of novel substituted-*N*-(6-(4-(pyrazine-2-carbonyl)piperazine/homopiperazine-1-yl)pyridin-3-yl)benzamide derivatives were designed, synthesized, and evaluated for their anti-tubercular activity against *Mycobacterium tuberculosis* H37Ra. Among the tested compounds, five compounds (**6a**, **6e**, **6h**, **6j** and **6k**) from Series-I and one compound (**7e**) from Series-II exhibited significant activity against *Mycobacterium tuberculosis* H37Ra with 50% inhibitory concentrations (IC_{50}) ranging from 1.35 to 2.18 μM. To evaluate the efficacy of these compounds, we examined their IC_{90} values. Five of the most active compounds were found to be more active with IC_{90}s ranging from 3.73 to 4.00 μM and one compound (**6e**) showed an IC_{90} of 40.32 μM. Moreover, single crystals were developed for **6d**, **6f** and **6n**. In addition, most active compounds were evaluated for their cytotoxicity on HEK-293 (human embryonic kidney) cells. Our results indicate that the compounds are nontoxic to human cells. The molecular interactions of the derivatised conjugates in docking studies reveal their suitability for further development.

1. Introduction

Tuberculosis (TB) is an infectious disease, caused by the Gram positive aerobic acid fast bacillus *Mycobacterium tuberculosis* (MTB) and it is one of the major cause of deaths. MDR-TB patients still develop resistance when treated with two of the most effective first-line drugs (rifampicin and isoniazid) along with second-line drugs such as the fluoroquinolones and injectable aminoglycoside or polypeptide drugs leading to extensively drug resistant TB. Hence there is an urgent need for new and effective anti-TB drugs.[1,2] Pyrazinamide (PZA) is well-known front line prodrug and is used in the treatment of active TB. New WHO guidelines recommend PZA for isoniazid-resistant and rifampicin susceptible tuberculosis for six months.[1] Reports reveal that the analogues of pyrazine and pyrazinamide can exhibit higher anti-TB activity against MTB.[3–16] Substituted *N*-phenylpyrazine-2-carboxamides synthesized by Dolezal *et al.* were evaluated *in vitro* for anti-mycobacterial activity. It was shown that compound *N*-(4-(trifluoromethyl)phenyl)pyrazine-2-carboxamide (**A**), *N*-(2-bromo-3-methylphenyl)pyrazine-2-carboxamide (**B**) and *N*-(3-iodo-4-methylphenyl)pyrazine-2-carboxamide (**C**) exhibited four times higher activity (MIC ≤ 2 μg L^{-1}) than the standard drug PZA (=8 μg L^{-1}).[17] 5-(*tert*-Butyl)-6-chloro-*N*-(3-iodo-4-methylphenyl)pyrazine-2-carboxamide (**D**), another active compound also showed high anti-mycobacterial activity with an IC_{50} of 0.728 μg mL^{-1}; IC_{90} = 0.819 μg mL^{-1} (PZA IC_{90} > 20 μg mL^{-1}).[17] Zhou *et al.* also reported PZA analogues of which *N*-(2-(piperazin-1-yl)ethyl)pyrazine-2-carboxamide (**E**) and *N*-(2-morpholinoethyl)pyrazine-2-carboxamide (**F**) were shown to exhibit MICs of 12.2 μg mL^{-1} and 8.0 μg mL^{-1} respectively against MTB H37Rv (Fig. 1).[18]

[a]*Department of Chemistry, Birla Institute of Technology and Science, Pilani, Hyderabad Campus, Jawahar Nagar, Kapra Mandal, Hyderabad-500078, Telangana, India. E-mail: kvgc@hyderabad.bits-pilani.ac.in; kvgcs.bits@gmail.com; Tel: +91 40 66303527*

[b]*Department of Green Chemistry and Technology, Faculty of Bioscience Engineering, Ghent University, Coupure Links 653, B-9000, Ghent, Belgium*

[c]*Department of Pharmacy, Birla Institute of Technology and Science, Pilani, Hyderabad Campus, Jawahar Nagar, Kapra Mandal, Hyderabad-500078, Telangana, India*

[d]*Medicinal Chemistry Research Laboratory, Department of Pharmacy, Birla Institute of Technology and Science, Pilani, 333031, India*

† Electronic supplementary information (ESI) available. CCDC 1979943–1979945. For ESI and crystallographic data in CIF or other electronic format see DOI: 10.1039/d0ra01348j

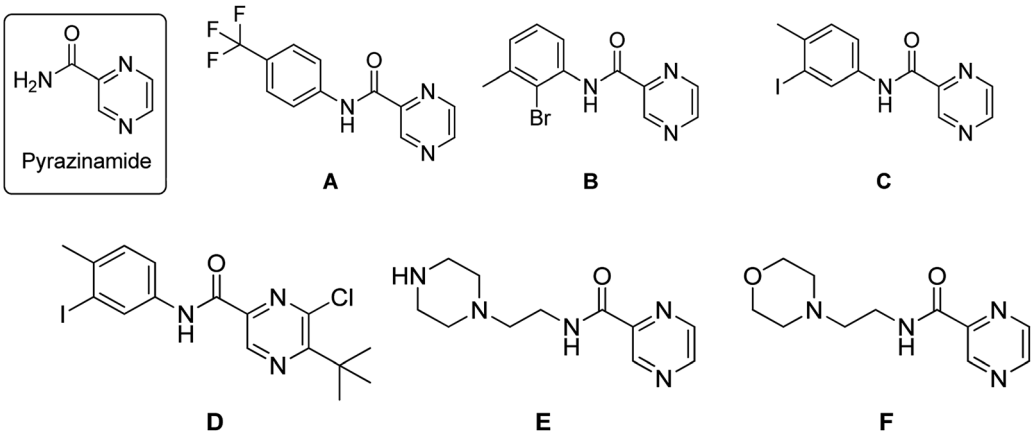

Fig. 1 Pyrazinamide based anti-tubercular agents.

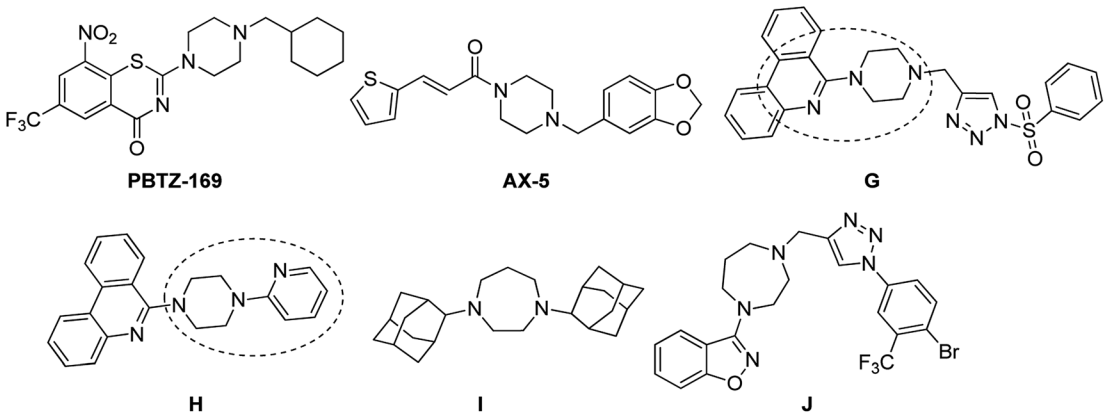

Fig. 2 Piperazine/homopiperazine based anti-tubercular agents.

Piperazine rings are a central core for several antibiotics which include ciprofloxacin, sparfloxacin, levofloxacin. PBTZ169 is a piperazine based clinical candidate which inhibits DprE1 and has synergic effect with either bedaquiline, clofazimine, delamanid or sutezolid.[19] AX-35 is another piperazine based potent anti-TB agent with MIC 0.3 μM against *M. bovis* BCG and MTB H37Rv targeting QcrB.[20] Bobesh *et. al.*, and Chandran *et. al.*, reported several piperazine based active anti-tubercular agents of which 4-(2-(7-methoxy-2-oxo-1,5-naphthyridin-1-(2*H*)-yl)ethyl)-*N*-(4-nitrophenyl)piperazine-1-carboxamide[21] and *N*-(4-chlorophenyl)-4-(6-nitro-4-oxo-4*H*-benzo[*e*][1,3]thiazin-2-yl)piperazine-1-carbothioamide[18] were the most active compounds with IC_{50} 0.29 μM and 0.51 μM in the DNA supercoiling assay and MTB MIC 3.45 μM and 4.41 μM respectively.[21,22] In our previous work, we linked a piperazine moiety to the pyridine nucleus of phenanthridine and these compounds were shown to exhibit good to excellent anti-TB activity with MICs ranging from 1.56 μg mL^{-1} to 50 μg mL^{-1}. Compounds 6-(4-((1-(phenylsulfonyl)-1*H*-1,2,3-triazol-4-yl)methyl)piperazin-1-yl)phenanthridine (**G**) and 6-(4-(pyridin-2-yl)piperazin-1-yl)phenanthridine (**H**) were the most active compounds with MTB MIC 1.56 μg mL^{-1} against H37Rv.[23,24] Compounds **I** and **J** are homo-piperazine based anti-TB agents with MIC 1.56 and 24.03 μM respectively[25,26] (Fig. 2). Few nicotine and nicotinamide based anti-TB agents are also reported in literature.[27–30] Recently Reddyrajula *et. al.*, reported several 1,2,3-triazole based pyrazine, pyrazinamide and nicotinamide analogues as good anti-TB agents and most of the compounds exhibited promising activity with MIC 1.56 μg mL^{-1} to 25.0 μg mL^{-1}.[30] Compound **K** is one of the most active nicotinamide analogue with MTB MIC 1.56 μg mL^{-1} (Fig. 3).

In our present work, we focused our efforts towards a synthetic strategy involving the incorporation of the active pharmacophore units of pyrazinamide, piperazine/homopiperazine and pyridine (Fig. 3) into one single molecule.

2. Results and discussion

Synthesis

As shown in Scheme 1, treatment of 2-chloro-5-nitropyridine (**1**) with 1-Boc-piperazine/1-Boc-homopiperazine at 110 °C yielded compounds **2a** and **2b**.[29] Intermediate compounds **2a** and **2b** were dissolved in CH_2Cl_2 and then treated with 4 N HCl in dioxane to get BOC protected compounds **3a** and **3b**. The amine compounds **3a** and **3b** were coupled with pyrazinoic acid using EDC·HCl, HOBt, *N*,*N*-diisopropylethylamine in DMF to yield

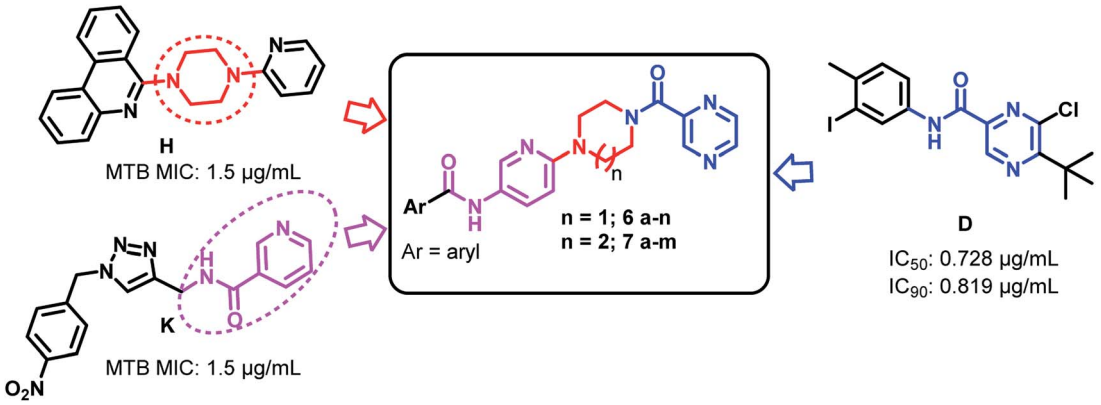

Fig. 3 Design of the titled compounds **6a–n** and **7a–m**.

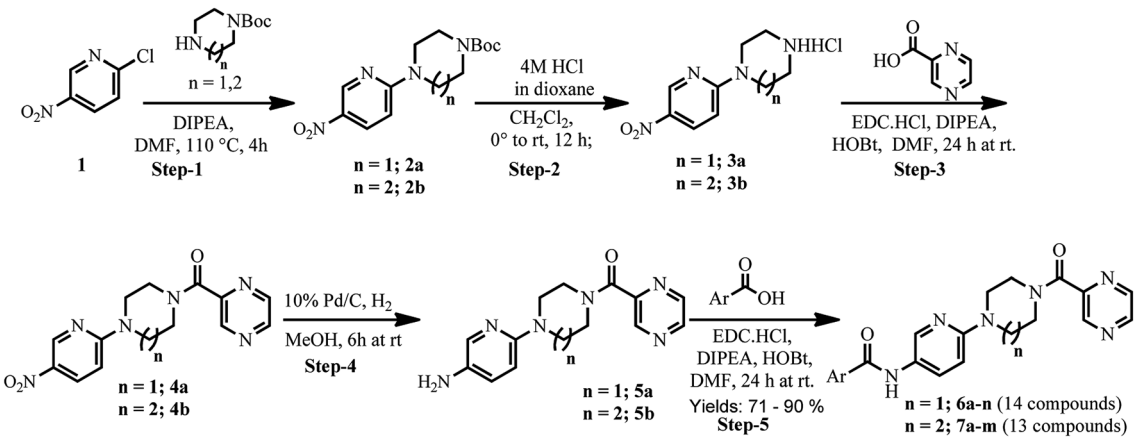

Scheme 1 Synthesis of titled compounds **6a–n** and **7a–m**.

compounds **4a** and **4b** respectively. Next, we prepared pre-final compounds **5a** and **5b** by reducing the nitro group of **4a** and **4b** with hydrogen gas in the presence of Pd catalyst. Finally, we performed acid–amine coupling by treating amines compounds **5a** and **5b** with different substituted benzoic acid, EDC·HCl, HOBt and *N*,*N*-diisopropylethylamine in DMF to yield the title compounds **6a–n** and **7a–m** respectively.

The purity of synthesized final compounds **6a–n** and **7a–m** was checked by LC-MS and elemental analyses. Structures of the compounds were confirmed by spectral data. In ^{1}H NMR and ^{13}C NMR, the signals of the corresponding protons and carbon atoms were verified on the basis of their chemical shifts, multiplicities, and coupling constants. The results of elemental analysis were within ±0.05 of the theoretical values.

^{1}H NMR of compounds from Scheme 1 showed singlets in the range 9.5 to 11 ppm due to amide proton and another singlet of triazole nucleus was observed between 8.5 to 9 ppm. Further, we observed a multiplet of eight protons in the aliphatic region (3 to 4.5 ppm) for **6a–n** and ten protons for compounds **7a–m**, confirming the presence of piperazine and homopiperazine respectively. All the compounds showed two peaks between 160 to 170 ppm in ^{13}C NMR indicating the presence of two amide carbons.

Biological activity

The pyrazinamide derivatives **6a–n** and **7a–m** were screened against the Gram-negative *Escherichia coli*, the Gram-positive *Staphylococcus aureus* and the acid-fast Mtb H37Ra. Results showed that the novel compounds maintained their specific antimicrobial activity against Mtb H37Ra as *E. coli* and *S. aureus* showed low susceptibility towards the final compounds, in contrast to the susceptibility of Mtb (Table 1). All compounds (**6a–n** and **7a–m**) were screened for their *in vitro* anti-TB activity towards Mtb H37Ra.[31] H37Ra is an attenuated tubercle bacillus strain closely related to the virulent type strain *M. tuberculosis* H37Rv. Several compounds significantly inhibited the growth at micro molar to submicromolar levels. We evaluated the IC_{50} and IC_{90} values for the final compounds. Among the twenty-seven compounds tested, eight compounds (**6a**, **6e**, **6h**, **6j**, **6k** and **7e**) exhibited excellent anti-mycobacterial activity against Mtb H37Ra with IC_{50} ranging from 1.35 μM to 2.18 μM and IC_{90} ranging from 3.73 μM to 40.32 μM as shown in Table 1.

Structure–activity relationship (SAR)

*SAR of substituted-N-(6-(4-(pyrazine-2-carbonyl)piperazin-1-yl) pyridin-3-yl)benzamide/isonicotinamide/pyrazine-2-carboxamide (**6a–n**).* Here, we evaluated fourteen compounds against *M.*

Table 1 Anti-mycobacterial activity of titled compound **6a–n** and **7a–m** against Mtb H37Ra

Entry	Ar	*n*	*S. aureus* IC_{50} (μM)	*E. coli* IC_{50} (μM)	*M. tuberculosis* H37Ra-lux IC_{50} (μM)	*M. tuberculosis* H37Ra-lux IC_{90} (μM)
Series-I						
6a		**1**	>64	>64	**1.46**	**3.73**
6b	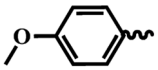	1	>64	>64	>64	>64
6c	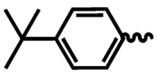	1	>64	>64	>64	>64
6d	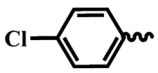	1	>64	>64	>64	>64
6e	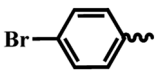	**1**	>64	>64	**2.18**	**40.32**
6f	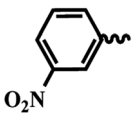	1	>64	>64	>64	>64
6g	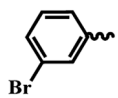	1	>64	>64	>64	>64
6h	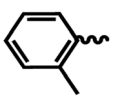	**1**	>64	>64	**1.82**	**3.85**
6i	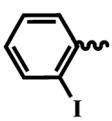	1	>64	>64	>64	>64
6j	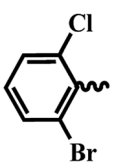	**1**	>64	>64	**2.14**	**3.94**
6k	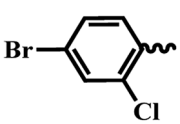	**1**	>64	>64	**1.35**	**4.00**
6l	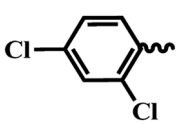	1	>64	>64	>64	>64
6m	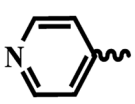	1	>64	>64	>64	>64
6n	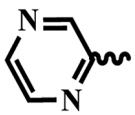	1	>64	>64	>64	>64

Table 1 (*Contd.*)

Entry	Ar	*n*	*S. aureus* IC_{50} (μM)	*E. coli* IC_{50} (μM)	*M. tuberculosis* H37Ra-lux IC_{50} (μM)	*M. tuberculosis* H37Ra-lux IC_{90} (μM)
Series-II						
7a	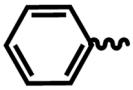	2	>64	>64	>64	>64
7b	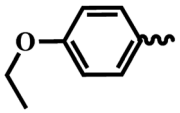	2	>64	>64	>64	>64
7c	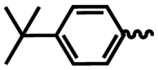	2	>64	>64	>64	>64
7d	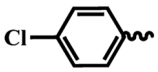	2	>64	>64	>64	>64
7e	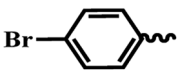	**2**	>64	>64	**2.12**	**3.88**
7f	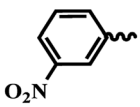	2	>64	>64	>64	>64
7g	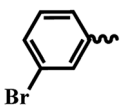	2	>64	>64	>64	>64
7h	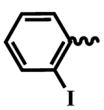	2	>64	>64	>64	>64
7i	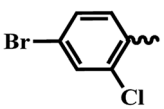	2	>64	>64	>64	>64
7j	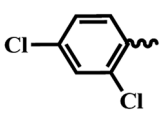	2	>64	>64	>64	>64
7k	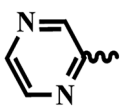	2	>64	>64	>64	>64
7l	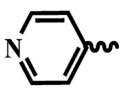	2	>64	>64	>64	>64
7m	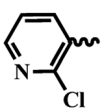	2	>64	>64	>64	>64
Doxycyclin	—	—	0.09	—	—	—
Norfloxacin	—	—	—	0.38	—	—
Isoniazid	—	—	—	—	0.013	—

tuberculosis H37Ra and SAR is explained on the basis of **6a**. Compound **6a** with no substituent on phenyl ring exhibited promising anti-TB activity with IC_{50} and IC_{90} 1.46 μM and 3.73 μM respectively. We introduced a strong electron donating group (–OMe), alkyl group (*t*-butyl) and halogen (Cl & Br) at the *para* position (**6b–e**) and noticed that the bromo substituted compound

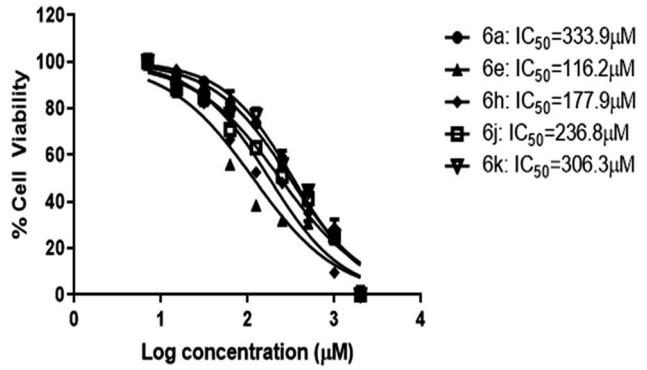

Fig. 4 IC_{50} results of the compounds by MTT assay. HEK-293 cells were treated with the compounds at concentrations ranging from 7–2000 μM ($n = 2$) for 24 h. Data represents mean ± SD.

6e exhibited good anti-TB activity with an IC_{50} of 2.18 μM and a moderate IC_{90} of 40.32 μM. *Meta*-substituted nitro compound **6f** and bromo-compound **6g** were inactive. *Ortho* substituted compound **6h** (methyl) is another potent anti-TB agent with IC_{50} and IC_{90} values of 1.82 μM and 3.82 μM respectively. Further, when we screened di-halogen substituted compounds **6j**, **6k** and **6l**, two of the derivatives with different halogens (Cl and Br) (**6j** and **6k**) exhibited good activity with MICs irrespective of their position while di-chloro compound (**6l**) was found to be inactive. With Cl and Br at *ortho* positions (**6j**), the IC_{50} and IC_{90} were 1.82 μM and 3.82 μM, whereas, bromo at *para* position and chloro at *ortho* position (**6k**) the IC_{50} and IC_{90} were 1.35 μM and 4.00 μM. When the phenyl group is replaced with a heterocyclic moiety (**6m** and **6n**) it resulted in loss of activity. In conclusion, from this series (**6a–n**), we noticed that unsubstituted phenyl (**6a**), *p*-bromo (**6e**), and *o*-methyl (**6h**) are well tolerated and compounds with three groups exhibited best activity. Di-halo substituted phenyl derivatives (**6j** and **6k**) were also found to be active against *M. tuberculosis* H37Ra.

*SAR of substituted-N-(6-(4-(homopyrazine-2-carbonyl)piperazin-1-yl)pyridin-3-yl)benzamide/isonicotinamide/pyrazine-2-carboxamide (**7a–m**).* Like piperazine analogues, various substituted homopiperazine analogues were also prepared. *Ortho*-, *para*- and *meta*-substituted derivatives, di-substituted halogen compounds and heterocyclic compounds were screened. Unfortunately, except the bromo-substituted compound (**7e**), all the other compounds were inactive (IC_{50} > 64 μM). In this series, *para* substituted bromo compound (**7e**) exhibited most potent activity with IC_{50} and IC_{90} values of 2.12 μM and 3.88 μM respectively.

Cytotoxicity studies

The most potent five compounds (**6a**, **6e**, **6h**, **6j** and **6k**) were subjected to cytotoxicity studies against normal human cell lines, human embryonic kidney (HEK) cells. Cell viability was measured by *in vitro* MTT assay.[32] Cells were exposed to compound treatment at of the following concentrations; 2000 μM, 1000 μM, 500 μM, 250 μM, 125 μM, 62.5 μM, 31.25 μM, 15.62 μM and 7.81 μM to determine their IC_{50} values from the dose–response curve. Data represent mean values of measurements ± SD (Fig. 4).

Docking studies

Docking studies were carried out using Schrödinger software[33] and the docking of significantly active molecules was performed using the Glide module[34] in Schrödinger. All docking calculations were performed using Extra Precision (XP) mode. A scaling factor of 0.8 and a partial atomic charge of less than 0.15 was applied to the atoms of the protein. The Glide docking score was used to determine the best-docked structure from the output. The interactions of these docked complexes were investigated further using XP visualizer.

In silico prediction of physico-chemical parameters

Physicochemical parameters of the designed compounds were *in silico* predicted using the QikProp module of Schrödinger. The different parameters predicted were; molecular weight (MW), total solvent accessible volume (TSAV), number of hydrogen bond donor (HBD), number of hydrogen bond acceptor (HBA), van der Waals polar surface area (PSA) of nitrogen and oxygen atoms, octanol/water partition coefficient (log *P*), aqueous solubility (log *S*), predicted apparent Caco-2 cell permeability in nm s^{-1} (P_{Caco}), apparent Madin Darby Canine Kidney (MDCK) permeability and percentage of human oral absorption.

Table 2 Principal descriptors predicted by QikProp

S. no.	Code	MW[a]	Volume[b]	Donor HB[c]	Accpt. HB[d]	PSA[e]
1	**6a**	388.43	1237.83	1	9.5	100.903
2	**6b**	418.45	1315.53	1	10.25	109.088
3	**6c**	444.54	1449.71	1	9.5	103.189
4	**6d**	422.87	1282.72	1	9.5	100.928
5	**6e**	467.32	1291.59	1	9.5	100.922
6	**6f**	433.43	1316.55	1	10.5	146.004
7	**6g**	467.32	1293.06	1	9.5	101.176
8	**6h**	402.46	1294.67	1	9.5	98.368
9	**6i**	514.33	1300.64	1	9.5	99.719
10	**6j**	501.77	1331.50	1	9.5	98.263
11	**6k**	501.77	1333.22	1	9.5	99.503
12	**6l**	457.32	1324.40	1	9.5	99.494
13	**6m**	389.42	1225.41	1	11	113.971
14	**6n**	390.40	1219.58	1	12	126.298
15	**7a**	402.46	1254.20	1	9.5	101.174
16	**7b**	446.51	1374.94	1	10.25	103.684
17	**7c**	458.56	1452.16	1	9.5	98.396
18	**7d**	436.90	1298.40	1	9.5	101.24
19	**7e**	481.35	1307.04	1	9.5	101.25
20	**7f**	447.45	1301.85	1	10.5	141.108
21	**7g**	481.35	1279.93	1	9.5	96.051
22	**7h**	528.35	1312.31	1	9.5	100.504
23	**7i**	515.80	1348.48	1	9.5	100.169
24	**7j**	471.35	1339.35	1	9.5	100.18
25	**7k**	404.43	1209.67	1	12	122.659
26	**7l**	403.44	1241.43	1	11	114.283
27	**7m**	454.89	1310.31	1	9.5	99.284

[a] Molecular weight, in Da (range for 95% of drugs: 130–725 Da). [b] Total solvent-accessible volume in cubic angstroms using a probe with a 1.4 Å radius (500–2000). [c] No. of hydrogen bonds donated by the molecule (range for 95% of drugs: 0–6). [d] No. of hydrogen bonds accepted by the molecule (range for 95% of drugs: 2–20). [e] van der Waals surface area of polar nitrogen and oxygen atoms (7–200).

Results and discussion of ADME parameters. Physico-chemical properties of a compound play a vital role in drug absorption, distribution metabolism and excretion. All the synthesized molecules were further evaluated for their drug-like behavior through ADME (absorption, distribution, metabolism and excretion) properties. Their molecular weights were <725 daltons with <6 hydrogen bond donors and <20 hydrogen bond acceptors (Table 2) fulfilling the criteria of Lipinski's rule of five and were found to be in the acceptable range for evaluation of the drug-like molecules. All other parameters, like octanol/water and solubility were also within the acceptable range. However, some compounds showed less predicted values of $P_{caco\text{-}2}$ permeability (compounds **6c**, **6f**, **6m**, **6n**, **7f**, **7k** and **7l**). Among the titled compounds, **6f** showed low Caco-2 cell membrane (Caco-2) permeability and percent human oral absorption with values of 63.37 nm s^{-1}, 57.59% respectively (Table 3). All the tested compounds showed more than 80% human intestinal oral absorption (except compounds **6f**, **6n**, **7f** and **7k**). Overall, the predicted physico chemical values indicate that a maximum number of titled analogues possessed the values that are well-matched with the optimum range values.

Molecular docking studies. The crystal structure of pantothenate synthetase[35] (PDB 3IUB) from *Mycobacterium tuberculosis* was retrieved from protein data bank[36] with a resolution of 1.5 Å. After importing the crystal structure into the work station of Schrödinger, the protein was prepared by protein preparation wizard and a grid was generated. The co-crystal ligand was extracted from the protein and re-docked in the generated grid and checked for the superimposition. The root mean square

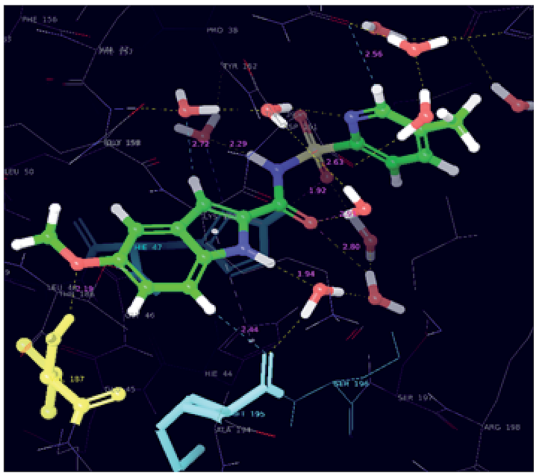

Fig. 5 Superimposed view of the native pose of ligand (X-ray crystallized pose) and docked pose of the same ligand in the active site of the protein (3IUB) (root mean square deviation 0.22 Å) (color interpretation – pink color – binding pose after docking, white color – X-ray native pose of ligand).

Table 3 Physico-chemical descriptors predicted by QikProp

S. no.	Code	log $P_{o/w}$[a]	log S[b]	P_{Caco}[c]	PMDCK[d]	Percent human oral absorption[e]
1	**6a**	2.617	−5.101	518.855	243.416	90.861
2	**6b**	2.716	−5.324	528.557	248.339	91.584
3	**6c**	3.71	−6.648	384.776	176.201	94.936
4	**6d**	3.106	−5.833	516.592	597.193	93.69
5	**6e**	3.181	−5.944	516.69	642.193	94.131
6	**6f**	1.939	−5.296	63.379	25.084	57.594
7	**6g**	3.19	−5.952	515.4	640.157	94.163
8	**6h**	3.036	−5.633	725.254	349.588	95.917
9	**6i**	3.271	−6	593.317	669.692	82.777
10	**6j**	3.661	−6.454	664.701	1490.213	85.946
11	**6k**	3.706	−6.608	647.779	1756.658	86.006
12	**6l**	3.631	−6.497	647.197	1632.012	100
13	**6m**	1.668	−4.415	278.843	124.409	80.479
14	**6n**	1.052	−4.03	184.188	79.466	73.651
15	**7a**	2.717	−4.828	525.517	246.796	91.549
16	**7b**	3.212	−5.149	906.183	444.739	100
17	**7c**	3.972	−6.094	859.818	420.196	100
18	**7d**	3.202	−5.552	525.206	607.987	94.385
19	**7e**	3.275	−5.66	523.982	652.031	94.791
20	**7f**	1.984	−4.505	105.505	43.514	61.814
21	**7g**	3.249	−5.191	873.968	1133.125	100
22	**7h**	3.294	−5.708	559.505	597.557	82.453
23	**7i**	3.758	−6.416	602.205	1614.986	85.746
24	**7j**	3.682	−6.301	601.965	1501.502	100
25	**7k**	1.146	−3.284	301.161	135.205	78.021
26	**7l**	1.767	−4.143	281.02	125.458	81.119
27	**7m**	3.422	−5.748	637.589	1033.633	100

[a] Predicted octanol/water partition co-efficient log P (acceptable range: −2.0 to 6.5). [b] Predicted aqueous solubility; S in mol L^{-1} (acceptable range: −6.5 to 0.5). [c] Apparent Caco-2 permeability (nm s^{-1}) (<25 poor, >500 great). [d] Apparent MDCK permeability (nm s^{-1}) (<25 poor, >500 great). [e] Percentage of human oral absorption (<25% poor and >80% is high).

Table 4 Docking interactions between amino acid residues, water molecules with the co-crystal ligand and significantly active compound

S. no.	Code	Hydrogen-bond	Aromatic bond	π–π interactions	Glide score (kcal mol^{-1})	Glide energy (kcal mol^{-1})
1	Co-crystal ligand (FG-2), (PDB 3IUB)	MET-40, HIS-47, VAL-187, H_2O bonds (**6**)	HIS-47, GLN-164, MET-195	HIS-44 (π–π stacking)	−9.6	−70.6
2	**6k**	H_2O	THR-276	ARG-198	−2.3	−32.10

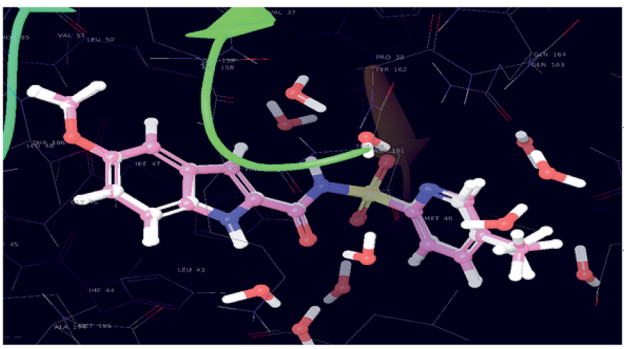

Fig. 6 Docked pose of co-crystallized ligand and its interactions in the active site of the protein-3IUB (color interpretation yellow – hydrogen bond, blue – aromatic bond).

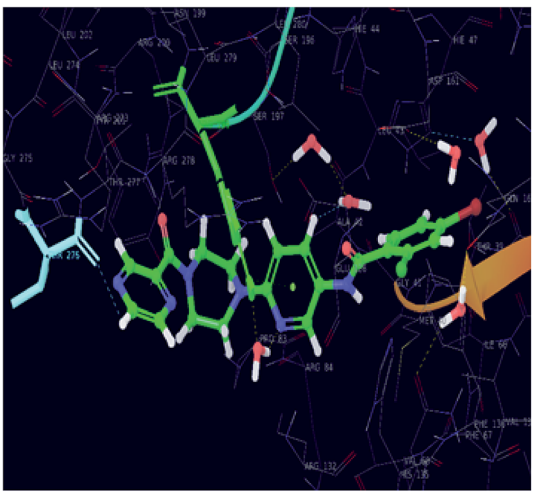

Fig. 7 2D representation of the docked pose of the co-crystallized ligand (color interpretation magenta – hydrogen bond, green – π–π stacking).

deviation (RMSD) was found to be 0.22 Å indicating that the docking protocol could be reliable for the study (Fig. 5).

Results and discussion of the molecular docking studies

In order to find the putative binding mode of the significantly active molecule, a docking study was carried out and the docked poses were analyzed using XP visualizer. The docked values along with their interactions are discussed in the Table 4. By scrutinizing the 3D and 2D (Fig. 6 and 7) poses of the co-crystal ligand, water molecules played a vital role in the hydrogen bond formation and formed six bonds. Amino acid residues MET-40, HIS-47 and VAL-187, contributed their part in the hydrogen bond formation with the co-crystal ligand and showed a docking score and energy of −9.6 and −70.6 kcal mol^{-1}, respectively. Apart from the hydrogen bond interactions, the co-crystal ligand also exhibited three aromatic bonds with the HIS-47, MET-195 and

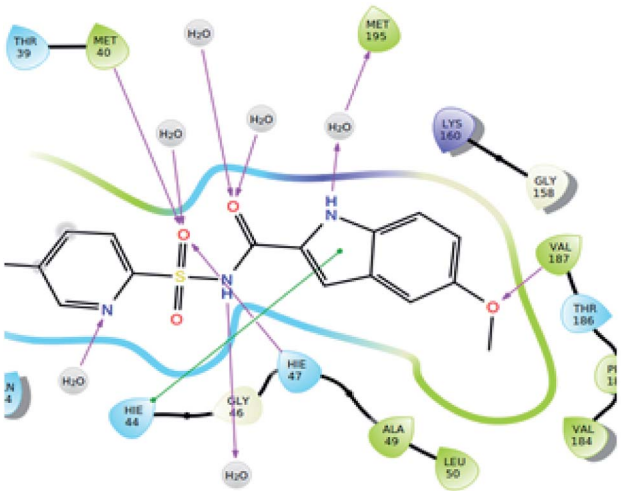

Fig. 8 Collaboration of the significantly active compound **6k** exhibiting various interactions in the active site of the protein (3IUB) (color interpretation yellow – hydrogen bond, blue – aromatic bond).

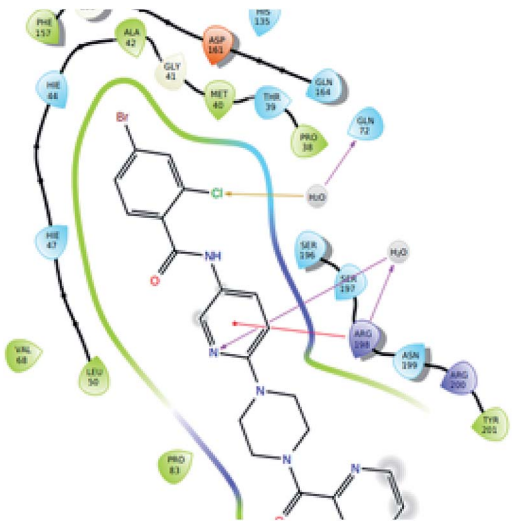

Fig. 9 2D representation of the docked pose of the significantly active compound **6k** (color interpretation magenta – hydrogen bond, red – π-cation and yellow – halogen bond).

Table 5 Crystal data and refinement parameters for **6d**, **6f** and **6n**

Identification code	**6d**	**6f**	**6n**
Empirical formula	$C_{21}H_{19}ClN_6O_2$	$C_{21}H_{19}N_7O_4$	$C_{19}H_{18}N_8O_2$
Formula weight	422.88	433.43	390.41
Temperature/K	100	100	100
Crystal system	Monoclinic	Triclinic	Monoclinic
Space group	$P2_1/n$	$P\bar{1}$	$P2_1/c$
a/Å	5.69780(10)	8.2628(2)	30.7919(5)
b/Å	21.2347(3)	9.9451(2)	5.80932(8)
c/Å	16.1672(2)	12.8729(3)	9.90381(15)
α/°	90	74.307(2)	90
β/°	98.5610(10)	74.059(2)	96.4675(15)
γ/°	90	79.348(2)	90
Volume/Å^3	1934.29(5)	972.22(4)	1760.32(5)
Z	4	2	4
ρ_{calc} g cm^{-3}	1.4520	1.481	1.473
μ/mm^{-1}	2.024	0.890	0.843
F(000)	884.1	452.0	816.0
Crystal size/mm^3	0.2 × 0.1 × 0.05	0.13 × 0.1 × 0.05	0.2 × 0.1 × 0.05
Radiation	Cu Kα (λ = 1.54184)	Cu Kα (λ = 1.54184)	Cu Kα (λ = 1.54184)
2Θ range for data collection/°	8.32 to 160.48	9.304 to 158.86	8.67 to 159.206
Index ranges	$-6 \le h \le 5$	$-6 \le h \le 10$	$-38 \le h \le 38$
	$-26 \le k \le 24$	$-12 \le k \le 12$	$-5 \le k \le 7$
	$-20 \le l \le 20$	$-11 \le l \le 16$	$-12 \le l \le 12$
Reflections collected	10 531	10 168	9609
Independent reflections	4009 [R_{int} = 0.0330, R_{sigma} = 0.0373]	4089 [R_{int} = 0.0215, R_{sigma} = 0.0248]	3735 [R_{int} = 0.0264, R_{sigma} = 0.0334]
Data/restraints/parameters	4009/0/271	4089/0/289	3735/0/316
Goodness-of-fit on F^2	1.028	1.061	1.028
Final R indexes [$I \ge 2\sigma(I)$]	R_1 = 0.0419, wR_2 = 0.1168	R_1 = 0.0365, wR_2 = 0.0980	R_1 = 0.0430, wR_2 = 0.1147
Final R indexes [all data]	R_1 = 0.0448, wR_2 = 0.1189	R_1 = 0.0382, wR_2 = 0.0996	R_1 = 0.0461, wR_2 = 0.1173

GLN-164 amino acid residues. HIS-44 amino acid residue revealed π–π stacking interaction with the co-crystal ligand.

The significantly active compound **6k** demonstrated a lower docking score when compared to the co-crystal ligand showing a docking score of −2.3 kcal mol^{-1} and docking energy of −32.10 kcal mol^{-1}. 3D picture of the compound **6k** (Fig. 8) showed the aromatic interaction with the amino acid residue THR-276. The pyridine nitrogen played an essential role in the hydrogen bond formation with the water molecule and in 2D representation (Fig. 9), chlorine atom which is present in the bromo benzene moiety actively participated in the halogen bond formation with a water molecule. *In vitro* studies of titled molecules revealed a correlation between the docking studies and most of the compounds were found to be less active.

X-ray crystallographic studies

Single crystal X-ray crystallographic structure of compounds 6d, 6f and 6n. The suitable crystals of compound **6d**, **6f** and **6n**, for single crystal X-ray diffraction (SCXRD) analysis were grown from the mixture of 40% methanol in dichloromethane. The SCXRD measurements were performed on the Rigaku XtaLAB P200 diffractometer using graphite monochromated Cu-Kα radiation (λ = 1.54184 Å). The data was collected and reduced using CrysAlisPro (Rigaku Oxford Diffraction) software. The data collection was carried out at 100 K and the structures were solved using Olex2 with the ShelX structure solution program using direct methods and refined with the ShelXL refinement package using least squares minimization. The details of the crystal data for all the three compounds is given in Table 5. The CCDC numbers for the structures of **6d**, **6f** and **6n** are 1979945, 1979944 and 1979943 respectively.

The structure of **6n** crystallizes in monoclinic $P2_1/c$ space group with $C_{19}H_{18}N_8O_2$ empirical formula. The terminal pyrazine ring in the structure is disordered over 2 positions with 0.60 and 0.40 occupancies. Moreover, the carbonyl oxygen adjacent to this pyrazine ring is also disordered over 2 positions with 0.34 and 0.66 occupancies (Fig. 10). However, such disorder was not observed in the case of compounds **6d** and **6f** with the empirical formulas $C_{22}H_{20}N_2O_2Cl$ and $C_{21}H_{19}N_7O_4$ and, respectively.

Interestingly, compounds **6d** and **6f** show intermolecular H-bonding through amidic C═O and N–H groups. Compound P9 **6d** displays intermolecular H-bonding. However, in this case each molecule is H-bonded to two more molecules through amidic oxygen and nitrogen atoms whereby amidic oxygen is H-bonded to one molecule whereas the amidic N–H is H-bonded to a second molecule. This results in each molecule being H-bonded to two other molecules as shown in Fig. 11. The H-bonding distance in this case is about 2.99 Å.

Similarly, in the case of **6n**, each ligand molecule is H-bonded to another ligand molecule through 2 hydrogen bonds. The H-bonding distance between N6 of one molecule and O1 of the other molecule is about 2.8 Å. This gives rise to AB stacking of the molecules when viewed along a-axis where

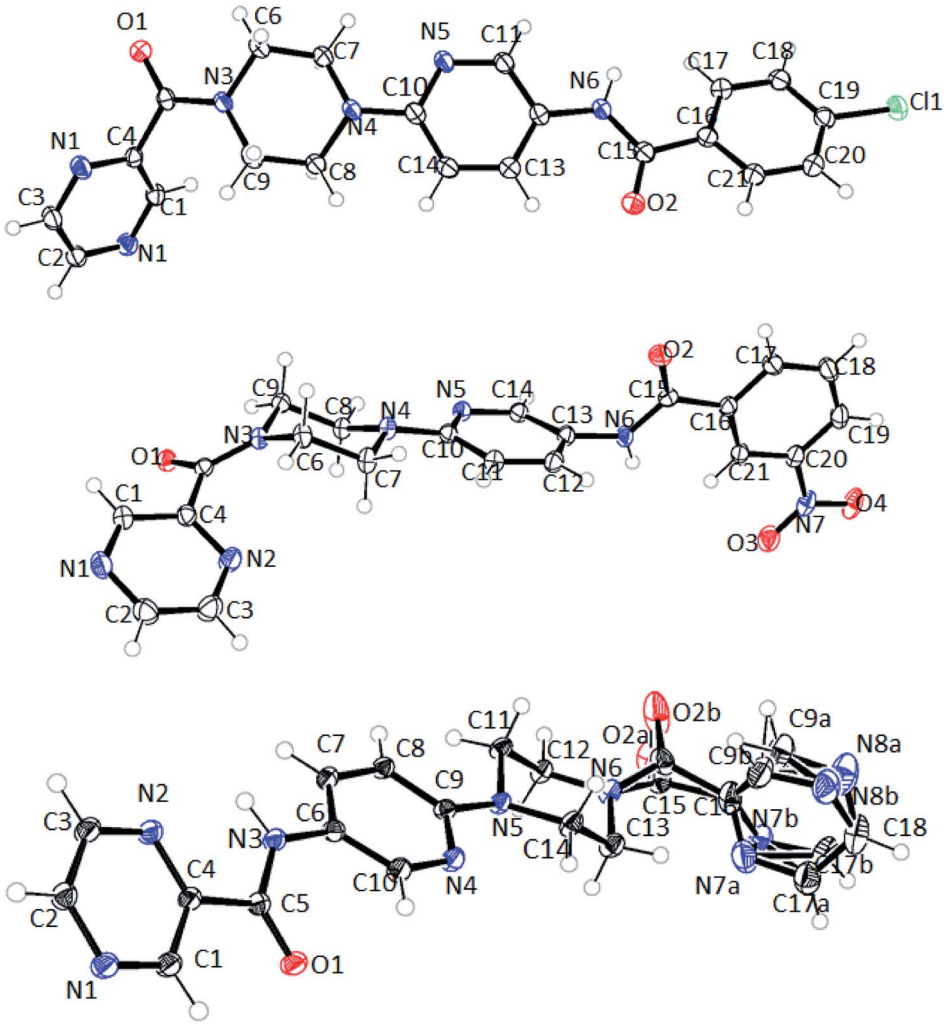

Fig. 10 ORTEP diagram of compound **6d** (top), **6f** (middle) and **6n** (bottom).

pyrazine rings of the molecules A and B point in opposite directions, thus resulting in the two molecules being non-superimposable upon each other (Fig. 12).

3. Conclusion

In conclusion, we identified five potential hit compounds from Series-I and one compound from Series-II. Compounds **6a**, **6e**, **6h**, **6j**, **6k** and **7k** exhibited greatest activity with IC_{50} values of 1.46, 2.18, 1.82, 2.14, 1.35 and 2.12 μM respectively and IC_{90} of 3.73, 40.32, 3.85, 3.94, 4.00 and 3.88 respectively against *M. tuberculosis* H37Ra. Further, docking studies were carried out for all the compounds using Schrödinger software and the docking of significantly active molecules was performed using the Glide module in Schrödinger. The most active compounds were found to be less toxic against HEK 298 cells. We developed single crystals for **6d**, **6f** and **6n**.

4. Experimental section

Materials and methods

Representative procedure for the synthesis of compounds 2a and 2b. A solution of 2-chloro-5-nitropyridine (**1**) (5.0 g, 31.53 mmol) in DMF, 1-Boc-piperazine/1-Boc-homopiperazine (6.4 g, 44.75 mmol) and *N*,*N*-diisopropylethylamine (16.5 mL, 94.9 mmol) was stirred for 4 h at 110 °C. Once completion of the reaction, as indicated by TLC, the reaction was quenched with cold water, solid was filtrated and washed with water and hexane to get the compound **2a** and **2b**.

*Compound **2a**.* Yellow solid (9.0 g, yield: 92%); melting point of **2a**: 168–170 °C; ESI-MS showed 309.16 $(M + H)^+$. ^{1}H NMR (400 MHz, DMSO) δ 8.97 (s, 1H), 8.25 (dd, $J = 9.6$, 2.9 Hz, 1H), 6.94 (d, $J = 9.6$ Hz, 1H), 3.83–3.72 (m, 4H), 3.51–3.41 (m, 4H), 1.43 (s, 9H).

*Compound **2b**.* Yellow solid (8.9 g, yield: 89%); melting point of **2b**: 157–159 °C; ESI-MS showed 323.20 $(M + H)^+$. ^{1}H NMR (400 MHz, DMSO) δ 8.97 (s, 1H), 8.21 (dd, $J = 9.2$, 2.6 Hz, 1H), 6.86 (d, $J = 9.6$ Hz, 1H), 4.05–3.65 (m, 4H), 3.63–3.43 (m, 2H), 3.33–3.30 (m, 2H), 1.77 (q, 2H), 1.25 (s, 9H).

Representative procedure for the synthesis of compound 3a and 3b. *tert*-Butyl 4-(5-nitropyridin-2-yl)piperazine-1-carboxylate/*tert*-butyl 4-(5-nitropyridin-2-yl)-1,4-diazepane-1-carboxylate (**2a**/**2b**) (9.0 g, 1.0 equiv.) was added in CH_2Cl_2 and cooled to 0 °C, after 5 min, 4 N HCl in dioxane (4.5 mL) was

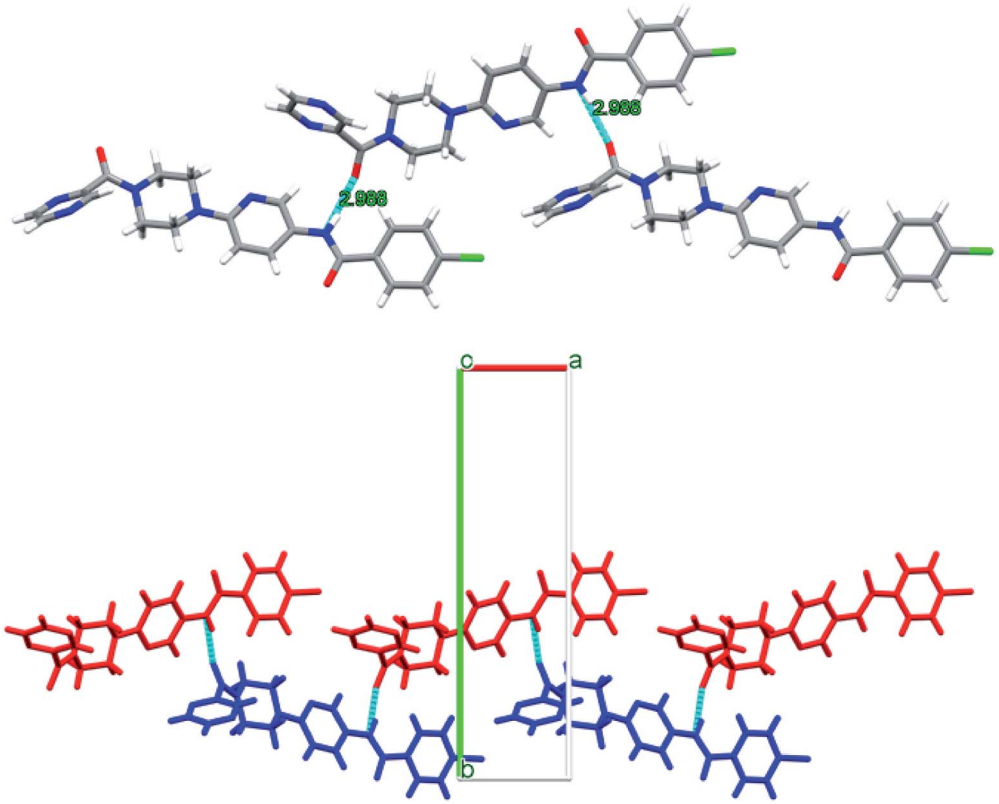

Fig. 11 Intermolecular H-bonding arrangement in compound **6d** (top) where C (grey), N (blue), O (red) and H (white), and packing arrangement in **6d** (bottom) along *c*-axis.

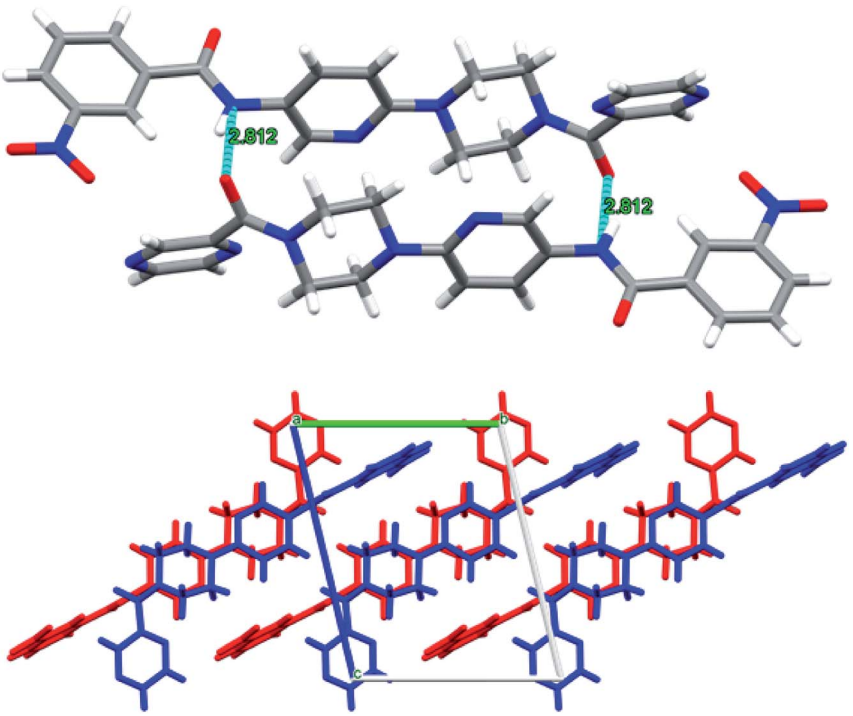

Fig. 12 Intermolecular H-bonding arrangement in **6f** (top) where C (grey), N (blue), O (red) and H (white), and view of H-bonded molecules along *a*-axis (bottom). The molecules A and B have been shown in red and blue colours for the ease of visualization.

added and warmed at rt for 12 h. After completion of the reaction, as indicated by TLC, the reaction was concentrated *in vacuo* and washed with *n*-pentane. Compounds **3a** and **3b** were obtained in excellent yield ~98% as yellow solids.

*Compound **3a**.* Pale yellow solid (7.1 g, yield: 98%); melting point of **3a**: 84–86 °C (salt free compound); ESI-MS showed 209.20 $(M + H)^+$. ^{1}H NMR (400 MHz, DMSO) δ 9.69 (bs, 2H), 8.99 (s, 1H), 8.39–8.22 (m, 1H), 7.04 (d, $J = 9.6$ Hz, 1H), 4.45–4.38 (m, 4H), 4.11–3.95 (m, 4H).

*Compound **3b**.* Pale yellow solid (7.20 g, yield: 100%); melting point of **3b**: 79–81 °C (salt free compound); ESI-MS showed 223.20 $(M + H)^+$. ^{1}H NMR (400 MHz, DMSO) δ 9.47 (bs, 2H), 8.99 (s, 1H), 8.27 (dd, $J = 9.6$, 2.8 Hz, 1H), 6.90 (d, $J = 9.6$ Hz, 1H), 3.93–3.96 (m, 4H), 3.34–3.07 (m, 4H), 2.12 (q, 2H).

Representative procedure for the synthesis of compounds 4a and 4b. EDC·HCl (1.20 equiv.) and *N*,*N*-diisopropylethylamine (2.5 equiv.) were added to a solution of compound **3a** (1 equiv.), pyrazinoic acid (1 equiv.) and HOBt (1.2 equiv.) in DMF and stirred for 24 h at room temperature under nitrogen. Once completion of the reaction, as indicated by TLC, the reaction was quenched with cold water and extracted with ethyl acetate. The organic layers were collected, washed with saturated brine solution, dried over anhydrous Na_2SO_4 and concentrated *in vacuo*. The resultant crude product was purified by column chromatography [ethyl acetate/hexane (30–40%)] to get the compound **4a** and **4b**.

*Compound **4a**.* Yellow gummy solid; yield: 83%; ESI-MS showed 315.16 $(M + H)^+$. ^{1}H NMR (400 MHz, DMSO) δ 8.91 (s, 1H), 8.61–8.52 (m, 3H), 8.11 (dd, $J = 9.6$, 2.9 Hz, 1H), 6.79 (d, $J = 9.6$ Hz, 1H), 3.88–3.63 (m, 4H), 3.50–3.08 (m, 4H).

*Compound **4b**.* Yellow gummy solid; yield: 73%; ESI-MS showed 329.20 $(M + H)^+$. ^{1}H NMR (400 MHz, DMSO) δ 8.92 (s, 1H), 8.67–8.56 (m, 3H), 8.17 (dd, $J = 9.6$, 2.9 Hz, 1H), 6.85 (d, $J = 9.6$ Hz, 1H), 3.83–3.71 (m, 4H), 3.60–3.03 (m, 4H), 1.78 (q, 2H).

Representative procedure for the synthesis of compounds 5a and 5b. To stirred suspension of an appropriate nitro compound **4a** (1 equiv.) and 10% Pd–C (0.2–0.3 g) in methanol. H_2 was added at a pressure 60 psi in hydrogenation shaker for 6 h at room temperature. Once completion of the reaction, as indicated by TLC, the reaction mixture was filtered through Celite and washed with excess of methanol. The combined filtrate washings were evaporated under reduced pressure. Crude residue was washed with hexane and diethyl ether to get compound **5a** and **5b** as solids. These two compounds were directly taken to next step without further purification.

*Compound **5a**.* Dark black and gummy solid; yield: 82%; ESI-MS showed 285.16 $(M + H)^+$.

*Compound **5b**.* Dark brown and gummy solid; yield: 70%; ESI-MS showed 399.20 $(M + H)^+$.

Representative procedure for the synthesis of compounds 6a–n. EDC·HCl (1.20 equiv.) and *N*,*N*-diisopropylethylamine (2.5 equiv.) were added to a solution of compound **5a** (1 equiv.), substituted benzoic acid (1.2 equiv.) and HOBt (1.2 equiv.) in DCM and stirred for 24 h at room temperature under nitrogen. Once completion of the reaction, as indicated by TLC, the reaction was quenched with cold water and extracted with DCM. The organic layers were collected, washed with saturated brine solution, dried over anhydrous Na_2SO_4 and concentrated *in vacuo*. The resultant crude product was purified by column chromatography [methanol/DCM (2–5%)] to get the compound **6.** Yields of **6a–n:** 65–93%. Similar procedure was followed to get the titled compounds **7a–m** from **5b**.

Biological assays

Antitubercular activity. In vitro anti-mycobacterial activity of the compounds was evaluated by a luminometric assay based on a *M. tuberculosis* H37Ra laboratory strain transformed with a pSMT1 luciferase reporter plasmid (H37Ra-lux). A twofold serial dilution of each compound was made in complete 7H9 broth with final concentrations ranging from 128 to 0.125 μm. Volumes of 100 μL of the serial dilutions were added in triplicate to black, flat-bottomed 96-well plates. As a positive control, isoniazid, a first-line anti-mycobacterial drug, was included. The mycobacterial suspension was made by thawing a frozen glycerol stock of H37Ra-lux and, subsequently, diluting it in complete H9 broth to obtain a suspension with 10 000 relative light units (RLU) per mL. A volume of 100 μL of bacteria was added to each well. All of the outer-perimeter wells were filled with 200 μL of sterile deionized water to minimize evaporation of the medium in the test wells during incubation. After 7 days, the bacterial replication was analyzed by luminometry. To evoke a luminescent signal, 25 μL of 1% *n*-decanal in ethanol was added to each well, where after light emission was measured.

Cytotoxicity assay (MTT assay). Cytotoxicity of the novel promising compounds was determined using MTT assay. 7.5×10^3 cells were seeded in 96 well plates and incubated for overnight to get the cells attached. Cells were treated with synthesized compounds at different concentrations (2000 μM, 1000 μM, 500 μM, 250 μM, 125 μM, 62.5 μM, 31.25 μM, 15.62 μM and 7.81 μM) in duplicates wells and incubated for 24 h. Then 50 μL of 5 mg mL^{-1} 3-(4,5-dimethylthiazol-2-yl)-2,5-diphenyltetrazolium bromide (MTT; Himedia Laboratories Pvt. Ltd., Mumbai, India) was added into each well on the next day and incubated for 4 h. The formed formazan crystals were dissolved using DMSO and absorbance was measured using Spectramax M4 (Molecular Devices, USA).

Cell culture and assay procedure. All the compounds were tested for their cytotoxicity against Human Embryonic Kidney (HEK) cell lines (procured from National Centre for Cell Science, Pune, India) that were cultured in DMEM (high glucose media: AL007S, Dulbecco's modified Eagle medium) with 10% fetal bovine serum (FBS) and 1% antibiotic (Pen–Strep: A001) incubated at 37 °C and 5% CO_2 atmosphere. All reagents were purchased from Himedia Laboratories Pvt. Ltd., Mumbai, India. Cells were seeded in a 96-well plate (Eppendorf 0030730119) with 100 μL of cell suspension containing 10^4 cells per well and incubated overnight. The stock DMSO solutions of the synthesized compounds and BG45 were prepared and they were further diluted to their respective concentrations of 2000 μM, 1000 μM, 500 μM, 250 μM, 125 μM, 62.5 μM, 31.25 μM, 15.62 μM and 7.81 μM with the DMEM complete media. The cells were then treated with 100 μL of the compound solutions made in media along with a blank control containing DMSO in medium and BG45 as positive control and were incubated for 24 h. The culture medium was aspirated and subsequently, 50 μL of 5 mg mL^{-1} concentrated solution of MTT (3-(4,5-dimethylthiazol-2-yl)-2,5-

diphenyltetrazolium bromide) in phenol red free DMEM was prepared and added into each well and further incubated for 4 h for the formation of formazan crystals. Later, 100 μL DMSO was added to the culture after aspirating media to dissolve the formazan crystals and the absorbance was measured using multi-well plate reader Spectramax (Molecular Devices, USA) at two different wavelengths of 570 nm and 650 nm. The % cell viability was calculated as a fraction of absorbance obtained from the treated cells over the absorbance of untreated control cells considering 100% cell viability in the blank control wells.[32]

Materials and methods of docking. Docking studies were carried out using Schrödinger software (Version 2019-1, Schrödinger) installed on Intel Xenon W 3565 processor and Ubuntu enterprise version 18.04 as the operating system. Targeted ligands were drawn in ChemDraw 18.0. The result of the docking results was analyzed with the help of XP Visualiser (Version 2019-1, Schrödinger).

Ligand preparation. The ligands used as inputs for docking were sketched using ChemDraw software and cleaned up the structure for the bond alignment; ligands were incorporated into the workstation, the energy was minimized using OPLS3e force field in Ligprep (Version 2019-1, Schrödinger). This minimization helps to assign bond orders, the addition of the hydrogens to the ligands and conversion of 2D to 3D structure for the docking studies. The generated output file (best conformations of the ligands) was used for docking studies.

Receptor grid generation. A receptor grid was generated around the protein by picking the inhibitory ligand (X-ray pose of the ligand in the protein). The centroid of the ligand is selected to create a grid box around it, and van der Waals radius of receptor atoms was scaled to 1.00 Å with a partial atomic charge of 0.25.

Protein preparation. Protein was prepared using the protein preparation wizard (Version 2019-1, Schrödinger). Hydrogen atom was added to the proteins and charges were assigned. Generated het states using Epik at pH 7.0 ± 2.0. Pre-process the protein and refine, modify the protein by analyzing the workspace, water molecules and other heteroatoms were examined and the non-significant atoms were excluded from the crystal structure of the protein. Finally, the protein was minimized using OPLS3e force filed. A grid was created by considering co-crystal ligand, which is included in the active site of the selected target pantothenate synthetase (PDB 3IUB) from *Mycobacterium tuberculosis*.

Chemistry. Chemicals and solvents were procured from commercial source. The solvents and reagents were of LR grade and if necessary purified before use. Thin-layer chromatography (TLC) was carried out on aluminum-supported silica gel plates (Merck 60 F254) with visualization of components by UV light (254 nm). Column chromatography was carried out on silica gel (Merck 100–200 mesh). ^{1}H NMR and ^{13}C NMR spectra were recorded at 400 MHz and 101 MHz respectively using a Bruker AV 400 spectrometer (Bruker Co., Switzerland) in $CDCl_3$ and DMSO-d_6 solution with tetramethylsilane as the internal standard and chemical shift values (δ) were given in ppm. Melting points were determined on an electro thermal melting point apparatus (Stuart-SMP30) in open capillary tubes and are uncorrected. Elemental analyses were performed by Elementar Analysensysteme GmbH vario MICRO cube CHN Analyzer.

Spectral data

Analytical data for the final compounds

*N-(6-(4-(Pyrazine-2-carbonyl)piperazin-1-yl)pyridin-3-yl)benzamide (**6a**).* Off white solid (88%); mp 137–139 °C; IR (KBr) ν_{max}/cm^{-1} 3573, 3032, 2923, 1675, 1445, 1052. ^{1}H NMR (400 MHz, DMSO-d_6) δ 10.17 (s, 1H), 8.90 (d, J = 1.5 Hz, 1H), 8.78 (d, J = 2.6 Hz, 1H), 8.71 (dd, J = 2.5, 1.5 Hz, 1H), 8.49 (d, J = 2.5 Hz, 1H), 8.03–7.90 (m, 3H), 7.64–7.49 (m, 3H), 6.91 (d, J = 9.1 Hz, 1H), 3.84–3.77 (m, 2H), 3.65–3.48 (m, 6H). ^{13}C NMR (101 MHz, DMSO-d_6) δ 165.7, 165.3, 156.0, 149.7, 146.0, 145.0, 143.7, 140.8, 135.0, 132.0, 131.7, 128.9, 128.0, 127.5, 107.5, 46.6, 45.9, 45.3, 41.90. EI-MS m/z 389.17 (M + H)$^+$; anal. calcd for $C_{21}H_{20}N_6O_2$: (%) C, 64.94; H, 5.20; N, 21.64; found: C, 64.95; H, 5.21; N, 21.65.

*4-Methoxy-N-(6-(4-(pyrazine-2-carbonyl)piperazin-1-yl)pyridin-3-yl)benzamide (**6b**).* White solid (87%); mp 188–190 °C; (KBr) ν_{max}/cm^{-1} 3579, 3029, 2853, 1687, 1408, 1344, 500. ^{1}H NMR (400 MHz, DMSO-d_6) δ 10.28 (s, 1H), 8.90 (d, J = 1.5 Hz, 1H), 8.79 (d, J = 2.6 Hz, 1H), 8.72 (dd, J = 2.6, 1.5 Hz, 1H), 8.49 (d, J = 2.6 Hz, 1H), 7.97–7.91 (m, 2H), 7.90 (s, 1H), 7.78–7.73 (m, 2H), 6.92 (d, J = 9.1 Hz, 1H), 3.83 (s, 3H), 3.81–3.76 (m, 2H), 3.63–3.48 (m, 6H). ^{13}C NMR (101 MHz, DMSO-d_6) δ 165.3, 165.1, 162.3, 155.9, 149.7, 146.0, 145.0, 143.7, 140.8, 131.7, 129.9, 127.7, 127.1, 114.0, 107.5, 55.9, 46.6, 46.0, 45.3, 41.9. EI-MS m/z 418.18 (M + H)$^+$; anal. calcd for $C_{22}H_{22}N_6O_2$: (%) C, 63.15; H, 5.31; N, 20.08; found: C, 63.17; H, 5.32; N, 20.09.

*4-(tert-Butyl)-N-(6-(4-(pyrazine-2-carbonyl)piperazin-1-yl)pyridin-3-yl)-benzamide (**6c**).* White solid (91%); mp 156–158 °C; IR (KBr) ν_{max}/cm^{-1} 3576, 3031, 2925, 1685, 1421, 1330, 1050. ^{1}H NMR (400 MHz, DMSO-d_6) δ 10.09 (s, 1H), 8.90 (d, J = 1.5 Hz, 1H), 8.78 (d, J = 2.6 Hz, 1H), 8.71 (dd, J = 2.5, 1.5 Hz, 1H), 8.48 (d, J = 2.6 Hz, 1H), 7.98–7.85 (m, 3H), 7.58–7.50 (m, 2H), 6.90 (d, J = 9.1 Hz, 1H), 3.81 (dd, J = 13.1, 8.4 Hz, 2H), 3.67–3.46 (m, 6H), 1.32 (s, 9H). ^{13}C NMR (101 MHz, DMSO-d_6) δ 165.3, 163.7, 152.1, 149.0, 146.2, 145.1, 143.7, 140.8, 134.1, 131.9, 131.7, 130.1, 127.3, 125.1, 107.5, 46.6, 45.9, 45.2, 41.9, 35.9, 30.8. EI-MS m/z 445.27 (M + H)$^+$; anal. calcd for $C_{25}H_{28}N_6O_2$: (%) C, 67.56; H, 6.35; N, 18.92; found: C, 67.57; H, 6.37; N, 18.93.

*4-Chloro-N-(6-(4-(pyrazine-2-carbonyl)piperazin-1-yl)pyridin-3-yl)-benzamide (**6d**).* Light yellow solid (81%); mp 144–146 °C; IR (KBr) ν_{max}/cm^{-1} 3585, 3031, 2922, 1675, 1532, 1372, 1027, 575. ^{1}H NMR (400 MHz, DMSO-d_6) δ 10.23 (s, 1H), 8.90 (d, J = 1.3 Hz, 1H), 8.78 (d, J = 2.5 Hz, 1H), 8.71 (dd, J = 2.4, 1.5 Hz, 1H), 8.47 (d, J = 2.5 Hz, 1H), 8.04–7.91 (m, 3H), 7.61 (d, J = 8.5 Hz, 2H), 6.91 (d, J = 9.1 Hz, 1H), 3.83–3.75 (m, 2H), 3.57 (ddd, J = 22.2, 7.7, 4.1 Hz, 6H). ^{13}C NMR (101 MHz, DMSO-d_6) δ 165.3, 164.6, 156.1, 149.7, 146.0, 145.0, 143.7, 140.8, 136.8, 133.7, 131.7, 130.1, 128.9, 127.3, 107.5, 46.6, 46.27–45.97 (m), 45.6, 41.9. EI-MS m/z 423.87 (M + H)$^+$; anal. calcd for $C_{21}H_{19}ClN_6O_2$: (%) C, 59.65; H, 4.54; N, 19.87; found: C, 59.66; H, 4.54; N, 19.88.

*4-Bromo-N-(6-(4-(pyrazine-2-carbonyl)piperazin-1-yl)pyridin-3-yl)-benzamide (**6e**).* White solid (90%); mp 119–121 °C; IR (KBr) ν_{max}/cm^{-1} 3590, 3021, 2843, 1687, 1410, 1340, 570. ^{1}H NMR (400 MHz, DMSO-d_6) δ 10.26 (s, 1H), 8.90 (d, J = 1.5 Hz, 1H), 8.78 (d, J = 2.6 Hz, 1H), 8.72 (dd, J = 2.6, 1.5 Hz, 1H), 8.47 (d, J = 2.6 Hz, 1H),

7.97–7.91 (m, 2H), 7.90 (s, 1H), 7.78–7.72 (m, 2H), 6.92 (d, J = 9.1 Hz, 1H), 3.81–3.76 (m, 2H), 3.64–3.48 (m, 6H). ^{13}C NMR (101 MHz, DMSO-d_6) δ 165.3, 164.7, 156.1, 149.7, 146.0, 145.0, 143.7, 140.8, 134.1, 131.9, 131.7, 130.1, 127.3, 125.8, 107.5, 46.6, 45.9, 45.3, 41.9. EI-MS m/z 468.08 $(M + H)^+$; 469.07 $(M + H)^{2+}$; anal. calcd for $C_{21}H_{19}BrN_6O_2$: (%) C, 53.97; H, 4.10; N, 17.98; found: C, 53.98; H, 4.11; N, 17.99.

*3-Nitro-N-(6-(4-(pyrazine-2-carbonyl)piperazin-1-yl)pyridin-3-yl)-benzamide (**6f**).* Yellow solid (82%); mp 202–203 °C; IR (KBr) ν_{max}/cm^{-1} 3590, 3021, 2833, 1515, 1679, 1410, 1340, 1120, 1061. ^{1}H NMR (400 MHz, DMSO-d_6) δ 10.52 (s, 1H), 8.90 (d, J = 1.2 Hz, 1H), 8.83–8.76 (m, 2H), 8.74–8.69 (m, 1H), 8.50 (d, J = 2.4 Hz, 1H), 8.47–8.39 (m, 2H), 7.96 (dd, J = 9.1, 2.5 Hz, 1H), 7.85 (t, J = 8.0 Hz, 1H), 6.94 (d, J = 9.1 Hz, 1H), 3.83–3.77 (m, 2H), 3.66–3.51 (m, 6H). ^{13}C NMR (101 MHz, DMSO-d_6) δ 165.4, 163.6, 156.2, 149.6, 148.2, 146.0, 144.9, 143.7, 140.9, 136.3, 134.5, 131.9, 130.7, 127.6, 126.7, 122.7, 107.5, 46.6, 45.8, 45.2, 41.9. EI-MS m/z 434.15 $(M + H)^+$; anal. calcd for $C_{21}H_{19}N_7O_4$: (%) C, 58.19; H, 4.42; N, 22.63; found: C, 58.20; H, 4.43; N, 22.64.

*3-Bromo-N-(6-(4-(pyrazine-2-carbonyl)piperazin-1-yl)pyridin-3-yl)-benzamide (**6g**).* White solid (76%); mp 246–248 °C; IR (KBr) ν_{max}/cm^{-1} 3595, 3059, 2933, 1680, 1412, 1357, 1279, 1045, 612. ^{1}H NMR (400 MHz, DMSO-d_6) δ 10.27 (s, 1H), 8.90 (d, J = 1.5 Hz, 1H), 8.78 (d, J = 2.6 Hz, 1H), 8.71 (dd, J = 2.5, 1.5 Hz, 1H), 8.48 (d, J = 2.6 Hz, 1H), 8.14 (t, J = 1.7 Hz, 1H), 8.00–7.90 (m, 2H), 7.80 (ddd, J = 8.0, 1.9, 0.9 Hz, 1H), 7.50 (t, J = 7.9 Hz, 1H), 6.92 (d, J = 9.1 Hz, 1H), 3.84–3.76 (m, 2H), 3.65–3.50 (m, 6H). ^{13}C NMR (101 MHz, DMSO-d_6) δ 165.3, 164.1, 156.1, 149.7, 146.0, 145.0, 143.7, 140.8, 137.1, 134.7, 131.7, 131.1, 130.6, 127.2, 122.2, 107.5, 46.6, 45.9, 45.2, 41.9. EI-MS m/z 467.09 $(M + H)^+$; 469.08 $(M + H)^{2+}$; anal. calcd for $C_{21}H_{19}BrN_6O_2$: (%) C, 53.98; H, 4.10; N, 17.98; found: C, 53.99; H, 4.11; N, 17.99.

*2-Methyl-N-(6-(4-(pyrazine-2-carbonyl)piperazin-1-yl)pyridin-3-yl)-benzamide (**6h**).* Brown solid (80%); mp 165–167 °C; IR (KBr) ν_{max}/cm^{-1} 3542, 3027, 2832, 1675, 1424, 1365, 1034, 1020. ^{1}H NMR (400 MHz, DMSO-d_6) δ 10.16 (s, 1H), 8.90 (s, 1H), 8.78 (d, J = 2.4 Hz, 1H), 8.71 (s, 1H), 8.47 (d, J = 2.3 Hz, 1H), 7.95 (dd, J = 9.0, 2.4 Hz, 1H), 7.46 (d, J = 7.4 Hz, 1H), 7.39 (t, J = 7.3 Hz, 1H), 7.34–7.25 (m, 2H), 6.90 (d, J = 9.1 Hz, 1H), 3.79 (d, J = 5.0 Hz, 2H), 3.63–3.55 (m, 4H), 3.50 (d, J = 2.8 Hz, 2H), 2.39 (s, 3H). ^{13}C NMR (101 MHz, DMSO-d_6) δ 168.0, 165.3, 155.9, 149.7, 146.0, 145.0, 143.7, 140.0, 137.4, 135.8, 131.0, 130.8, 130.1, 127.8, 127.7, 126.1, 107.7, 46.6, 46.1, 45.4, 41.9, 19.8. EI-MS m/z 403.20 $(M + H)^+$; anal. calcd for $C_{22}H_{22}N_6O_2$: (%) C, 65.66; H, 5.52; N, 20.89; found: C, 65.67; H, 5.53; N, 20.90.

*2-Iodo-N-(6-(4-(pyrazine-2-carbonyl)piperazin-1-yl)pyridin-3-yl)-benzamide (**6i**).* White solid (89%); mp 165–167 °C; (KBr) ν_{max}/cm^{-1} 3599, 3027, 2834, 1677, 1412, 1343, 1043, 615. ^{1}H NMR (400 MHz, DMSO-d_6) δ 10.29 (s, 1H), 8.90 (d, J = 1.3 Hz, 1H), 8.78 (d, J = 2.5 Hz, 1H), 8.74–8.69 (m, 1H), 8.44 (d, J = 2.4 Hz, 1H), 7.97–7.90 (m, 2H), 7.50 (q, J = 7.2 Hz, 2H), 7.26–7.20 (m, 1H), 6.92 (d, J = 9.1 Hz, 1H), 3.83–3.77 (m, 2H), 3.63–3.55 (m, 4H), 3.53–3.48 (m, 2H). ^{13}C NMR (101 MHz, DMSO-d_6) δ 168.0, 165.3, 155.9, 146.0, 145.0, 143.7, 140.0, 137.4, 135.8, 131.0, 130.8, 130.0, 127.8, 127.3, 122.3, 107.7, 93.8, 46.6, 46.1, 45.4, 41.9. EI-MS m/z 515.08 $(M + H)^+$; anal. calcd for $C_{21}H_{19}IN_6O_2$: (%) C, 49.05; H, 3.73; N, 16.34; found: C, 49.07; H, 3.75; N, 16.35.

*2-Bromo-6-chloro-N-(6-(4-(pyrazine-2-carbonyl)piperazin-1-yl)-pyridin-3-yl)benzamide (**6j**).* P-7 pale yellow solid (87%); mp 150–152 °C; IR (KBr) ν_{max}/cm^{-1} 3582, 3022, 2973, 1671, 1422, 1332, 1055, 680. ^{1}H NMR (400 MHz, DMSO-d_6) δ 10.46 (s, 1H), 8.90 (d, J = 1.3 Hz, 1H), 8.78 (d, J = 2.5 Hz, 1H), 8.71 (dd, J = 2.5, 1.5 Hz, 1H), 8.42 (d, J = 2.6 Hz, 1H), 7.91 (dd, J = 9.1, 2.7 Hz, 1H), 7.84 (d, J = 2.4 Hz, 1H), 7.71 (dd, J = 8.6, 2.4 Hz, 1H), 7.53 (d, J = 8.6 Hz, 1H), 6.92 (d, J = 9.1 Hz, 1H), 3.82–3.78 (m, 2H), 3.64–3.55 (m, 4H), 3.53–3.49 (m, 2H). ^{13}C NMR (101 MHz, DMSO-d_6) δ 165.3, 163.5, 156.2, 149.7, 146.0, 145.0, 143.7, 139.9, 138.9, 134.3, 132.2, 131.9, 130.8, 129.9, 127.2, 120.4, 107.7, 46.6, 45.9, 45.3, 41.9. EI-MS m/z 501.04 $(M + H)^+$; 503.06 $(M + H)^{2+}$; anal. calcd for $C_{21}H_{18}BrClN_6O_2$: (%) C, 50.27; H, 3.64; N, 16.75; found: C, 50.28; H, 3.65; N, 16.76.

*4-Bromo-2-chloro-N-(6-(4-(pyrazine-2-carbonyl)piperazin-1-yl)-pyridin-3-yl)benzamide (**6k**).* Light brown solid (80%); mp 147–149 °C; IR (KBr) ν_{max}/cm^{-1} 3575, 30 311, 2925, 1673, 1402, 1043, 560. ^{1}H NMR (400 MHz, DMSO-d_6) δ 10.46 (s, 1H), 8.90 (s, 1H), 8.78 (d, J = 2.3 Hz, 1H), 8.71 (s, 1H), 8.42 (d, J = 2.2 Hz, 1H), 7.91 (dd, J = 9.0, 2.3 Hz, 1H), 7.84 (d, J = 2.1 Hz, 1H), 7.71 (dd, J = 8.5, 2.1 Hz, 1H), 7.54 (d, J = 8.6 Hz, 1H), 6.92 (d, J = 9.1 Hz, 1H), 3.80 (s, 2H), 3.66–3.54 (m, 5H), 3.51 (d, J = 4.6 Hz, 2H). ^{13}C NMR (101 MHz, DMSO-d_6) δ 165.4, 161.8, 156.2, 148.7, 148.2, 147.0, 145.4, 145.0, 144.7, 143.9, 143.8, 141.0, 131.7, 126.6, 107.4, 46.6, 45.7, 45.2, 41.8. EI-MS m/z 501.04 $(M + H)^+$; 503.06 $(M + H)^{2+}$; anal. calcd for $C_{21}H_{18}BrClN_6O_2$: (%) C, 50.27; H, 3.64; N, 16.75; found: C, 50.28; H, 3.65; N, 16.76.

*2,4-Dichloro-N-(6-(4-(pyrazine-2-carbonyl)piperazin-1-yl)pyridin-3-yl)benzamide (**6l**).* Off solid (80%); mp 197–199 °C; IR (KBr) ν_{max}/cm^{-1} 3595, 3029, 2945, 1683, 1422, 1053, 560. ^{1}H NMR (400 MHz, DMSO-d_6) δ 10.49 (s, 1H), 8.95 (d, J = 1.5 Hz, 1H), 8.88 (d, J = 2.5 Hz, 1H), 8.73 (dd, J = 2.6, 1.5 Hz, 1H), 8.46 (d, J = 2.6 Hz, 1H), 7.89 (dd, J = 9.1, 2.7 Hz, 1H), 7.80 (d, J = 2.4 Hz, 1H), 7.69 (dd, J = 8.6, 2.4 Hz, 1H), 7.49 (d, J = 8.6 Hz, 1H), 6.92 (d, J = 9.1 Hz, 1H), 3.78 (t, J = 5.2 Hz, 2H), 3.60–3.49 (m, 6H). ^{13}C NMR (101 MHz, DMSO-d_6) δ 165.4, 161.8, 156.2, 148.7, 148.2, 147.0, 145.4, 145.0, 144.7, 143.9, 143.8, 141.0, 131.7, 126.6, 107.4, 46.6, 45.7, 45.2, 41.8. EI-MS m/z 558.10 $(M + H)^+$; anal. calcd for $C_{21}H_{18}Cl_2N_6O_2$: (%) C, 55.16; H, 3.97; N, 18.38; found: C, 55.18; H, 3.98; N, 18.39.

*N-(6-(4-(Pyrazine-2-carbonyl)piperazin-1-yl)pyridin-3-yl) isonicotinamide (**6m**).* Off white solid (83%); mp 212–213 °C; IR (KBr) ν_{max}/cm^{-1} 3510, 3021, 2865, 1670, 1410, 1340, 1060. ^{1}H NMR (400 MHz, DMSO-d_6) δ 10.72 (s, 1H), 8.93 (d, J = 2.5 Hz, 2H), 8.91 (d, J = 1.6 Hz, 2H), 8.80 (dd, J = 2.5, 1.7 Hz, 2H), 8.78 (d, J = 2.6 Hz, 1H), 8.70 (dd, J = 2.6, 1.5 Hz, 1H), 8.66 (d, J = 2.7 Hz, 1H), 8.07 (dd, J = 9.1, 2.7 Hz, 1H), 6.90 (d, J = 9.1 Hz, 1H), 3.79 (dd, J = 6.6, 4.2 Hz, 2H), 3.63 (dd, J = 6.6, 4.2 Hz, 2H), 3.60–3.53 (m, 4H). ^{13}C NMR (101 MHz, DMSO-d_6) δ 166.5, 162.9, 156.1, 149.7, 146.1, 145.3, 145.1, 143.7, 143.6, 140.9, 131.2, 126.2, 121.2, 107.5, 46.7, 45.8, 45.1, 41.9. EI-MS m/z 389.19 $(M + H)^+$; anal. calcd for $C_{21}H_{20}N_6O_2$: (%) C, 64.94; H, 5.19; N, 21.64; found: C, 64.95; H, 5.21; N, 21.65.

*N-(6-(4-(Pyrazine-2-carbonyl)piperazin-1-yl)pyridin-3-yl)pyrazine-2-carboxamide (**6n**).* Off white solid (87%); mp 205–206 °C; (KBr) ν_{max}/cm^{-1} 3525, 3025, 2867, 16 775, 1412, 1363, 1022. ^{1}H NMR (400 MHz, DMSO-d_6) δ 10.73 (s, 1H), 10.73 (s, 1H), 9.28 (d, J =

1.5 Hz, 1H), 8.93 (d, J = 2.5 Hz, 1H), 8.90 (d, J = 1.5 Hz, 1H), 8.80 (dd, J = 2.5, 1.5 Hz, 1H), 8.78 (d, J = 2.6 Hz, 1H), 8.71 (dd, J = 2.5, 1.5 Hz, 1H), 8.63 (d, J = 2.6 Hz, 1H), 8.32 (d, J = 1.5 Hz, 1H), 8.07 (dd, J = 9.1, 2.7 Hz, 1H), 6.92 (d, J = 9.1 Hz, 1H), 3.82–3.77 (m, 2H), 3.67–3.50 (m, 7H). ^{13}C NMR (101 MHz, DMSO-d_6) δ 165.3, 161.9, 156.1, 149.7, 148.1, 146.0, 145.4, 145.0, 144.4, 143.7, 143.7, 141.0, 131.6, 126.6, 107.4, 46.6, 45.8, 45.2, 41.9. EI-MS m/z 391.16 (M + H)$^+$; anal. calcd for $C_{19}H_{18}N_8O_2$: (%) C, 58.45; H, 4.65; N, 28.70; found: C, 58.46; H, 4.67; N, 28.71.

*N-(6-(4-(Pyrazine-2-carbonyl)-1,4-diazepan-1-yl)pyridin-3-yl)benzamide (**7a**).* White solid (86%); mp 147–149 °C; IR (KBr) ν_{max}/cm^{-1} 3610, 3019, 2917, 1668, 1484, 1326, 1032. ^{1}H NMR (400 MHz, DMSO-d_6) δ 10.36 (s, 1H), 8.91 (d, J = 1.5 Hz, 1H), 8.76 (d, J = 2.6 Hz, 1H), 8.71 (dd, J = 2.6, 1.5 Hz, 1H), 8.47 (d, J = 2.8 Hz, 1H), 7.97–7.91 (m, 3H), 7.90 (s, 1H), 7.78–7.72 (m, 2H), 6.92 (d, J = 9.2 Hz, 1H), 3.71–3.66 (m, 8H), 2.44–2.18 (m, 2H). ^{13}C NMR (101 MHz, DMSO-d_6) δ 165.8, 163.7, 152.2, 148.9, 147.9, 145.2, 143.6, 140.7, 134.5, 131.9, 131.7, 130.2, 127.8, 125.8, 107.7, 67.3, 56.4, 52.1, 49.1, 29.7. EI-MS m/z 403.19 (M + H)$^+$; anal. calcd for $C_{22}H_{22}N_6O_2$: (%) C, 65.66; H, 5.51; N, 20.88; found: C, 65.67; H, 5.52; N, 20.89.

*4-Ethoxy-N-(6-(4-(pyrazine-2-carbonyl)-1,4-diazepan-1-yl)pyridin-3-yl)-benzamide (**7b**).* Brown solid (88%); mp 207–209 °C; IR (KBr) ν_{max}/cm^{-1} 3560, 3021, 2835, 1684, 1411, 1365, 1024. ^{1}H NMR (400 MHz, DMSO-d_6) δ 10.19 (s, 1H), 8.98 (d, J = 1.6 Hz, 1H), 8.73 (d, J = 2.5 Hz, 2H), 8.57 (d, J = 2.6 Hz, 1H), 7.90 (dd, J = 9.2, 2.3 Hz, 3H), 7.10–7.01 (m, 2H), 6.90 (d, J = 9.0 Hz, 1H), 4.15–4.07 (m, 2H), 3.79–3.75 (m, 4H), 3.60–3.54 (m, 4H), 3.50–3.45 (m, 2H), 1.31 (t, J = 7.0, 1.5 Hz, 3H). ^{13}C NMR (101 MHz, DMSO-d_6) δ 165.3, 165.2, 161.6, 155.6, 149.7, 146.1, 145.0, 143.7, 140.2, 132.0, 129.9, 127.7, 126.9, 114.5, 107.8, 63.9, 58.8, 55.4, 46.6, 46.0, 45.4, 41.3, 28.1, 15.0. EI-MS m/z 446.21 (M + H)$^+$; anal. calcd for $C_{24}H_{26}N_6O_3$: (%) C, 64.57; H, 5.87; N, 18.82; found: C, 64.58; H, 5.88; N, 18.83.

*4-(tert-Butyl)-N-(6-(4-(pyrazine-2-carbonyl)-1,4-diazepan-1-yl)-pyridin-3-yl)benzamide (**7c**).* Off white solid (83%); mp 228–230 °C; IR (KBr) ν_{max}/cm^{-1} 3573, 3029, 2912, 1672, 1420, 1335, 1066. ^{1}H NMR (400 MHz, DMSO-d_6) δ 10.21 (s, 1H), 8.93 (d, J = 1.5 Hz, 1H), 8.78 (d, J = 2.6 Hz, 1H), 8.71 (dd, J = 2.6, 1.5 Hz, 1H), 8.57 (d, J = 2.6 Hz, 1H), 7.87–7.91 (m, 2H), 7.91 (s, 1H), 7.76–7.70 (m, 2H), 6.91 (d, J = 9.1 Hz, 1H), 3.68–3.62 (m, 8H), 2.54–2.38 (m, 2H), 1.43 (s, 9H). ^{13}C NMR (101 MHz, DMSO-d_6) δ 166.2, 164.6, 153.1, 148.9, 145.8, 145.0, 143.9, 141.1, 134.2, 131.7, 131.2, 130.2, 127.7, 125.4, 107.7, 67.3, 55.4, 53.8, 46.9, 38.7, 35.1, 30.2, 25.6. EI-MS m/z 458.25 (M + H)$^+$; anal. calcd for $C_{26}H_{30}N_6O_2$: (%) C, 68.11; H, 6.59; N, 18.33; found: C, 68.13; H, 6.60; N, 18.34.

*4-Chloro-N-(6-(4-(pyrazine-2-carbonyl)-1,4-diazepan-1-yl)pyridin-3-yl)benzamide (**7d**).* White solid (77%); mp 240–242 °C; IR (KBr) ν_{max}/cm^{-1} 3575, 3039, 2940, 1684, 1412, 13 495, 1188, 1021, 782. ^{1}H NMR (400 MHz, DMSO-d_6) δ 10.21 (s, 1H), 8.76–8.65 (m, 2H), 8.64 (dd, J = 9.1, 2.8 Hz, 1H), 8.00–7.58 (m, 3H), 7.55–7.51 (m, 2H), 6.72 (dd, J = 9.2, 2.4 Hz, 1H), 3.84–3.50 (m, 8H), 1.93 (q, 2H). ^{13}C NMR (101 MHz, DMSO-d_6) δ 165.5, 164.8, 156.2, 149.8, 146.4, 145.5, 143.1, 140.8, 136.8, 133.7, 131.8, 129.2, 128.4, 127.7, 107.5, 55.9, 53.4, 50.7, 47.8, 25.8. EI-MS m/z 436.14 (M + H)$^+$; anal. calcd for $C_{22}H_{21}ClN_6O_2$: (%) C, 60.48; H, 4.84; N, 19.25; found: C, 60.49; H, 4.85; N, 19.50.

*4-Bromo-N-(6-(4-(pyrazine-2-carbonyl)-1,4-diazepan-1-yl)pyridin-3-yl)benzamide (**7e**).* White solid (90%); mp 119–121 °C; IR (KBr) ν_{max}/cm^{-1} 3590, 3021, 2843, 1687, 1410, 1340, 570. ^{1}H NMR (400 MHz, DMSO-d_6) δ 10.15 (s, 1H), 8.79–8.68 (m, 2H), 8.65 (dd, J = 9.1, 2.8 Hz, 1H), 8.42–8.34 (m, 1H), 7.98–7.90 (m, 2H), 7.89 (m, 1H), 7.79–7.74 (m, 2H), 6.73 (dd, J = 9.2, 2.4 Hz, 1H), 3.85–3.52 (m, 8H), 1.96 (q, 2H). ^{13}C NMR (101 MHz, DMSO-d_6) δ 166.7, 166.6, 164.6, 154.5, 150.4, 150.1, 145.9, 144.3, 143.5, 141.4, 134.2, 132.1, 131.9, 130.1, 125.8, 125.6, 105.7, 48.4, 47.7, 46.2, 45.2, 29.5. EI-MS m/z 481.19 (M + H)$^+$; 483.21 (M + H)$^{2+}$; anal. calcd for $C_{22}H_{21}BrN_6O_2$: (%) C, 54.91; H, 4.40; N, 17.46; found: C, 54.93; H, 4.42; N, 17.47.

*3-Nitro-N-(6-(4-(pyrazine-2-carbonyl)-1,4-diazepan-1-yl)pyridin-3-yl)benzamide (**7f**).* Yellow solid (78%); mp 212–213 °C; IR (KBr) ν_{max}/cm^{-1} 3591, 3041, 2893, 1689, 1411, 1351, 1120, 1061. ^{1}H NMR (400 MHz, DMSO-d_6) δ 10.32 (s, 1H), 8.90–8.76 (m, 2H), 8.63 (s, 1H) 8.51–8.32 (m, 4H) 7.97–7.90 (m, 2H), 6.73 (d, J = 9.3 Hz, 1H), 3.85–3.32 (m, 8H), 1.97 (p, 2H). ^{13}C NMR (101 MHz, DMSO-d_6) δ 171.3, 168.1, 159.4, 154.9, 153.0, 150.6, 149.0, 148.2, 146.1, 141.3, 139.2, 136.8, 135.4, 131.3, 127.5, 110.55, 53.32, 52.8, 59.0, 50.0, 29.3. EI-MS m/z 447.18 (M + H)$^+$; anal. calcd for $C_{22}H_{21}N_7O_4$: (%) C, 59.05; H, 4.73; N, 21.91; found: C, 58.20; H, 4.43; N, 22.64.

*3-Bromo-N-(6-(4-(pyrazine-2-carbonyl)-1,4-diazepan-1-yl)pyridin-3-yl) benzamide (**7g**).* White solid (71%); mp 246–248 °C; IR (KBr) ν_{max}/cm^{-1} 3590, 3050, 2931, 1682, 1410, 1333, 1276, 1035, 615. ^{1}H NMR (400 MHz, DMSO-d_6) δ 10.29 (s, 1H), 8.87 (d, J = 1.6 Hz, 1H), 8.76 (d, J = 2.6 Hz, 1H), 8.70 (dd, J = 2.6, 1.6 Hz, 1H), 8.49 (d, J = 2.6 Hz, 1H), 8.24 (t, J = 1.8 Hz, 1H), 7.99–7.90 (m, 2H), 7.83 (ddd, J = 8.0, 2.0, 1.0 Hz, 1H), 7.54 (t, J = 7.9 Hz, 1H), 6.93 (d, J = 9.1 Hz, 1H), 3.57 3–3.50 (m, 4H), 3.45–3.37 (m, 6H), 1.85 (p, 2H). ^{13}C NMR (101 MHz, DMSO-d_6) δ 171.5, 168.3, 159.3, 155.1, 154.9, 152.9, 150.5, 149.1, 148.1, 141.2, 139.1, 136.9, 135.2, 131.3, 130.1, 127.6, 110.4, 53.1, 52.6, 51.8, 50.1, 30.0. EI-MS m/z 480.09 (M + H)$^+$; 482.08 (M + H)$^{2+}$; anal. calcd for $C_{22}H_{21}BrN_6O_2$: (%) C, 54.91; H, 4.40; N, 17.46; found: C, 54.92; H, 4.41; N, 17.48.

*2-Iodo-N-(6-(4-(pyrazine-2-carbonyl)-1,4-diazepan-1-yl)pyridin-3-yl)benzamide (**7h**).* Off white solid (80%); mp 226–228 °C; IR (KBr) ν_{max}/cm^{-1} 3581, 3032, 2916, 1689, 1417, 1325, 1130, 1060, 634. ^{1}H NMR (400 MHz, DMSO-d_6) δ 10.19 (s, 1H), 8.92 (d, J = 1.5 Hz, 1H), 8.88 (d, J = 2.6 Hz, 1H), 8.80–8.71 (m, 2H), 7.95 (dd, J = 9.0, 2.7 Hz, 2H), 7.49 (dd, J = 8.5, 6.6 Hz, 1H), 7.35 (d, J = 7.6 Hz, 2H), 6.91 (d, J = 9.1 Hz, 1H), 3.82–3.78 (m, 2H), 3.59 (t, 4H), 3.50–3.41 (m, 2H), 1.77 (p, 2H). ^{13}C NMR (101 MHz, DMSO-d_6) δ 168.0, 165.3, 155.9, 146.0, 145.0, 143.7, 139.9, 137.4, 135.8, 131.0, 130.8, 130.1, 127.8, 127.3, 122.3, 107.7, 93.8, 57.0, 53.2, 50.9, 47.2, 25.9. EI-MS m/z 528.17 (M + H)$^+$; anal. calcd for $C_{22}H_{21}IN_6O_2$: (%) C, 50.01; H, 4.02; N, 15.91; found: C, 50.03 H, 4.04; N, 15.92.

*4-Bromo-2-chloro-N-(6-(4-(pyrazine-2-carbonyl)-1,4-diazepan-1-yl)pyridin-3-yl)benzamide (**7i**).* White solid (77%); mp 221–223 °C; IR (KBr) ν_{max}/cm^{-1} 3560, 3029, 2864, 1686, 1415, 1323, 1109, 1031, 623. ^{1}H NMR (400 MHz, DMSO-d_6) δ 10.25 (s, 1H), 8.87–8.76 (dd, J = 2.6, 1.5 Hz, 2H), 8.52 (s, 1H), 7.90 (dd, J = 9.1, 2.7 Hz, 1H), 7.87 (d, J = 2.4 Hz, 1H), 7.69 (dd, J = 8.6, 2.4 Hz, 1H), 7.57 (d, J = 8.6 Hz, 1H), 6.73 (d, J = 9.1 Hz, 1H), 3.80–3.41

(m, 8H), 1.73 (p, 2H). ^{13}C NMR (101 MHz, DMSO-d_6) δ 165.4, 161.8, 156.2, 148.7, 148.2, 147.0, 145.4, 145.0, 144.7, 143.9, 143.8, 140.9, 131.7, 126.6, 107.4, 57.0, 53.2, 50.9, 47.2, 29.8. EI-MS m/z 514.06 $(M + H)^+$; 516.08 $(M + H)^{2+}$; anal. calcd for $C_{22}H_{20}BrClN_6O_2$: (%) C, 51.23; H, 3.92; N, 16.29; found: C, 51.24; H, 3.93; N, 16.30.

*2,4-Dichloro-N-(6-(4-(pyrazine-2-carbonyl)-1,4-diazepan-1-yl) pyridin-3-yl)benzamide (**7j**).* Off white solid (80%); mp 197–199 °C; IR (KBr) ν_{max}/cm^{-1} 3597, 3028, 2947, 1687, 1427, 1023, 569. ^{1}H NMR (400 MHz, DMSO-d_6) δ 10.36 (s, 1H), 8.89 (m. 2H), 8.78 (d, J = 2.5 Hz, 1H), 8.73 (dd, J = 2.6, 1.5 Hz, 1H), 87.89–7.5 (m, 3H), 7.42 (m, 1H), 7.78 (d, J = 2.4 Hz, 1H), 7.51 (d, J = 8.8 Hz, 1H), 6.90 (d, J = 9.0 Hz, 1H), 3.89–3.36 (m, 8H), 1.71 (p, 2H). ^{13}C NMR (101 MHz, DMSO-d_6) δ 165.4, 161.8, 156.2, 148.7, 148.2, 147.0, 145.4, 146.0, 145.7, 143.9, 143.8, 141.0, 132.9, 126.7, 109.4, 58.9, 54.2, 51.9, 48.2, 32.8. EI-MS m/z 470.12 $(M + H)^+$; anal. calcd for $C_{22}H_{20}Cl_2N_6O_2$: (%) C, 56.06; H, 4.28; N, 17.83; found: C, 56.08; H, 4.29; N, 17.84.

*N-(6-(4-(Pyrazine-2-carbonyl)-1,4-diazepan-1-yl)pyridin-3-yl) pyrazine-2-carboxamide (**7k**).* Brown solid (79%); mp 135–136 °C; IR (KBr) ν_{max}/cm^{-1} 3572, 3021, 2915, 1677, 1454, 1350, 1090. ^{1}H NMR (400 MHz, DMSO-d_6) δ 10.67 (s, 1H), 9.30 (d, J = 1.6 Hz, 1H), 8.94 (d, J = 2.7 Hz, 1H), 8.89 (d, J = 1.5 Hz, 1H), 8.81 (dd, J = 2.5, 1.7 Hz, 1H), 8.75 (d, J = 2.6 Hz, 1H), 8.70 (dd, J = 2.6, 1.7 Hz, 1H), 8.64 (d, J = 2.6 Hz, 1H), 8.17 (dd, J = 9.1, 2.7 Hz, 1H), 6.90 (d, J = 9.1 Hz, 1H), 3.66–3.60 (m, 8H), 2.47–2.28 (m, 2H). ^{13}C NMR (101 MHz, DMSO-d_6) δ 165.5, 162.0, 157.0, 149.8, 148.2, 146.2, 145.3, 145.2, 144.7, 143.3, 143.0, 140.6, 130.1, 126.6, 109.1, 67.3, 56.4, 52.8, 49.9, 28.7. EI-MS m/z 405.17 $(M + H)^+$; anal. calcd for $C_{20}H_{20}N_8O_2$: (%) C, 59.40; H, 4.98; N, 27.71; found: C, 59.42; H, 4.90; N, 27.72.

*N-(6-(4-(Pyrazine-2-carbonyl)-1,4-diazepan-1-yl)pyridin-3-yl) isonicotinamide (**7l**).* White solid (82%); mp 139–141 °C; IR (KBr) ν_{max}/cm^{-1} 3585, 3029, 2840, 1684, 1415, 1342, 1070. ^{1}H NMR (400 MHz, DMSO-d_6) δ 10.73 (s, 1H), 8.93 (d, J = 2.5 Hz, 2H), 8.91 (d, J = 1.6 Hz, 2H), 8.81 (dd, J = 2.5, 1.7 Hz, 2H), 8.78 (d, J = 2.5 Hz, 1H), 8.70 (dd, J = 2.6, 1.6 Hz, 1H), 8.66 (d, J = 2.7 Hz, 1H), 8.07 (dd, J = 9.1, 2.5 Hz, 1H), 6.89 (d, J = 9.2 Hz, 1H), 3.69–3.51 (m, 2H), 3.51 (t, 2H), 3.40–3.33 (m, 6H), 1.88 (p, 2H). ^{13}C NMR (101 MHz, DMSO-d_6) δ 166.5, 162.9, 156.0, 149.7, 146.3, 145.3, 145.1, 143.7, 143.6, 140.9, 131.2, 126.2, 121.2, 107.5, 67.3, 55.4, 53.8, 46.9, 25.6. EI-MS m/z 404.18 $(M + H)^+$; anal. calcd for $C_{21}H_{21}N_7O_2$: (%) C, 62.53; H, 5.25; N, 24.31; found: C, 62.54; H, 5.26; N, 24.33.

*2-Chloro-6-fluoro-N-(6-(4-(pyrazine-2-carbonyl)-1,4-diazepan-1-yl)pyridin-3-yl)benzamide (**7m**).* Off white solid (81%); mp 198–199 °C; IR (KBr) ν_{max}/cm^{-1} 3594, 3042, 2913, 1687, 1412, 1036, 654. ^{1}H NMR (400 MHz, DMSO-d_6) δ 10.32 (s, 1H), 8.90 (d, J = 1.6 Hz, 1H), 8.80 (d, J = 2.5 Hz, 1H), 8.74 (dd, J = 2.6, 1.6 Hz, 1H), 8.50 (d, J = 2.6 Hz, 1H), 7.61–7.44 (m, 4H), 6.92 (d, J = 9.1 Hz, 1H), 3.67–3.52 (m, 4H), 3.55–3.47 (m, 6H), 1.87 (p, 2H). ^{13}C NMR (101 MHz, DMSO-d_6) δ 165.7, 164.6, 159.3, 156.2, 149.6, 146.3, 145.1, 143.4, 141.8, 137.8, 136.7, 135.7, 131.2, 129.2, 128.1, 127.2, 113.2, 58.2, 56.2, 52.9, 46.2, 30.8. EI-MS m/z 454.14 $(M + H)^+$; anal. calcd for $C_{22}H_{20}ClFN_6O_2$: (%) C, 58.09; H, 4.43; N, 18.49; found: C, 58.10; H, 4.44; N, 18.50.

Conflicts of interest

There are no conflicts of interest to declare.

Acknowledgements

KVGCS and SM thank DBT, New Delhi [BT/IN/Spain/39/SMl2017-18] for providing financial support. The financial assistance provided by DST FIST grant (SR/FST/CSI-240/2012), New Delhi is gratefully acknowledged. SS thanks CSIR for providing SRF fellowship. Central analytical lab facilities of BITS Pilani Hyderabad campus are gratefully acknowledged.

References

1 https://apps.who.int/iris/bitstream/handle/10665/311389/9789241550529-eng.pdf.
2 https://www.atsjournals.org/doi/full/10.1164/rccm.167.4.603#readcube-epdf.
3 W. J. Chung, A. Kornilov, B. H. Brodsky, M. Higgins, T. Sanchez, L. B. Heifets, M. H. Cynamon and J. Welch, *Tuberculosis*, 2008, **88**, 410.
4 V. Judge, B. Narasimhan and M. Ahuja, *Hygeia*, 2012, **4**, 1.
5 M. Dolezal, P. Cmedlova, L. Palek, J. Vinsova, J. Kunes, V. Buchta, J. Jampilek and K. Kralova, *Eur. J. Med. Chem.*, 2008, **43**, 1105.
6 F. M. Vergara, C. H. Lima, M. D. Henriques, A. L. Candéa, M. C. Lourenço, L. M. Ferreira, C. R. Kaiser and M. V. de Souza, *Eur. J. Med. Chem.*, 2009, **44**, 4954.
7 D. Sriram, P. Yogeeswari and S. P. Reddy, *Bioorg. Med. Chem. Lett.*, 2006, **16**, 2113.
8 A. Imramovský, S. Polanc, J. Vinsová, M. Kocevar, J. Jampílek, Z. Recková and J. Kaustová, *Bioorg. Med. Chem.*, 2007, **15**, 2551.
9 M. Dolezal, L. Palek, J. Vinsova, V. Buchta, J. Jampilek and K. Kralova, *Molecules*, 2006, **11**, 242.
10 L. Semelková, O. Janďourek, K. Konečná, P. Paterová, L. Navrátilová, F. Trejtnar, V. Kubíček, J. Kuneš, M. Doležal and J. Zitko, *Molecules*, 2017, **22**, E495.
11 B. Servusová, J. Vobicková, P. Paterová, V. Kubíček, J. Kuneš, M. Doležal and J. Zitko, *Bioorg. Med. Chem. Lett.*, 2013, **23**, 3589.
12 N. R. Gangarapu, A. Ranganatham, E. K. Reddy, H. D. Surendra, A. M. Sajith, S. Yellappa and K. B. Chandrasekhar, *J. Heterocycl. Chem.*, 2019, **56**, 1117.
13 B. Servusova-Vanaskova, O. Jandourek, P. Paterova, J. Kordulakova, P. Magdalena, K. Vladimir Kubicek, R. Kucera, V. Garaj, L. Naesens, J. Kunes, M. Dolezala and J. Zitko, *RSC Med. Chem.*, 2015, **6**, 1311.
14 T. Stringer, R. Seldon, N. Liu, D. F. Warner, C. Tam, W. Cheng, L. M. Land, P. J. Smith, K. Chibale and G. S. Smith, *Dalton Trans.*, 2017, **46**, 9875.
15 J. Zitko, O. Jand'ourek, P. Paterová, L. Navrátilová, J. Kuneš, J. Vinšová and M. Doležal, *RSC Med. Chem.*, 2018, **9**, 685.
16 B. Servusová, P. Paterová, J. Mandíková, V. Kubíček, R. Kučera, J. Kuneš, M. Doležal and J. Zitko, *Bioorg. Med. Chem. Lett.*, 2014, **24**, 450.

17 M. Dolezal, J. Zitko, D. Kesetovicová, J. Kunes and M. Svobodová, *Molecules*, 2009, **14**, 4180.
18 S. Zhou, S. Yang and G. Huang, *J. Enzyme Inhib. Med. Chem.*, 2017, **32**, 1183.
19 A. Lupien, A. Vocat, C. S. Foo, E. Blattes, J. Y. Gillon, V. Makarov and S. T. Cole, *Antimicrob. Agents Chemother.*, 2018, **62**, e00840.
20 C. S. Foo, A. Lupien, M. Kienle, A. Vocat, A. Benjak, R. Sommer, D. A. Lamprecht, A. J. C. Steyn, K. Pethe, J. Piton, K. H. Altmann and S. T. Cole, *mBio*, 2018, **9**, e01276.
21 K. A. Bobesh, J. Renuka, R. R. Srilakshmi, S. Yellanki, P. Kulkarni, P. Yogeeswari and D. Sriram, *Bioorg. Med. Chem.*, 2016, **24**, 42.
22 M. Chandran, J. Renuka, J. P. Sridevi, G. S. Pedgaonkar, V. Asmitha, P. Yogeeswari and D. Sriram, *Int. J. Mycobact.*, 2015, **4**, 104.
23 H. N. Nagesh, K. M. Naidu, D. H. Rao, J. P. Sridevi, D. Sriram, P. Yogeeswari and K. V. G. Chandra Sekhar, *Bioorg. Med. Chem. Lett.*, 2013, **23**, 6805.
24 H. N. Nagesh, N. Suresh, K. M. Naidu, B. Arun, J. P. Sridevi, D. Sriram, P. Yogeeswari and K. V. G. Chandra Sekhar, *Eur. J. Med. Chem.*, 2014, **74**, 333.
25 E. Bogatcheva, C. Hanrahan, B. Nikonenko, R. Samala, P. Chen, J. Gearhart, F. Barbosa, L. Einck, C. A. Nacy and M. Protopopova, *J. Med. Chem.*, 2006, **49**, 3045.
26 K. M. Naidu, S. Srinivasarao, N. Agnieszka, A. K. Ewa, M. M. Kumar and K. V. G. Chandra Sekhar, *Bioorg. Med. Chem. Lett.*, 2016, **26**, 2245.
27 P. T. Gandhi, N. T. Athmaram and G. R. Arunkumar, *Bioorg. Med. Chem.*, 2016, **24**, 1637.
28 M. M. Patel and M. T. Chhabriya, *Am. J. Infect. Dis.*, 2011, **7**, 61.
29 P. C. Ting, J. F. Lee, N. Zorn, H. M. Kim, R. G. Aslanian, M. Lin, M. Smith, S. S. Walker, J. Cook, M. Van Heek and J. Lachowicz, *Bioorg. Med. Chem. Lett.*, 2013, **23**, 985.
30 R. Reddyrajula and U. Dalimba, *Bioorg. Med. Chem. Lett.*, 2020, **30**, 126846.
31 E. Torfs, J. Vajs, M. B. de Macedo, F. Cools, B. Vanhoutte, Y. Gorbanev, A. Bogaerts, L. Verschaeve, G. Caljon, L. Maes, P. Delputte, P. Cos, J. Košmrlj and D. Cappoen, *Chem. Biol. Drug Des.*, 2018, **91**, 631.
32 T. Prakruti, N. Adhikari, S. A. Amin, T. Jha and B. Ghosh, *Eur. J. Pharm. Sci.*, 2018, **124**, 165.
33 *Schrödinger Release 2019-1*, Maestro, Schrödinger, LLC, New York, NY, 2019.
34 R. A. Friesner, J. L. Banks, R. B. Murphy, T. A. Halgren, J. J. Klicic, D. T. Mainz, M. P. Repasky, E. H. Knoll, M. Shelley and J. K. Perry, *J. Med. Chem.*, 2004, **47**, 1739.
35 A. w. Hung, H. L. Silvestre, S. Wen, A. Ciulli, T. L. Blundell and C. Abell, *Angew. Chem., Int. Ed.*, 2009, **48**, 8452.
36 S. K. Burley, H. M. Berman, C. Bhikadiya, C. Bi, L. Chen, L. Di Costanzo, C. Christie, K. Dalenberg, J. M. Duarte and S. Dutta, *Nucleic Acids Res.*, 2019, **47**, 464.